



Schiff bases of 1'-hydroxy-2'-acetonaphthone containing chalcogen functionalities and their complexes with and (*p*-cymene)Ru(II), Pd(II), Pt(II) and Hg(II): Synthesis, structures and applications in C–C coupling reactions

Arun Kumar, Monika Agarwal, Ajai K. Singh *

Department of Chemistry, Indian Institute of Technology, New Delhi 110 016, India

ARTICLE INFO

Article history:

Received 25 April 2008

Received in revised form 19 July 2008

Accepted 22 July 2008

Available online 29 July 2008

Keywords:

Chalcogenated Schiff bases

Platinum metals

Synthesis

Crystal structure

Heck reaction

Suzuki reaction

ABSTRACT

Schiff bases of 1'-hydroxy-2'-acetonaphthone (HAN) containing chalcogen functionalities, 1-HO-C₁₀H₆-2-CH₃C=N-(CH₂)_nEC₆H₄-4-R (R = H or OMe; n = 2 or 3; E = S (L¹–L²), Se (L³–L⁴) or Te (L⁵–L⁶)) have been synthesized in yield 90–95%. They show characteristic ¹H, ¹³C{¹H}, ⁷⁷Se{¹H} and ¹²⁵Te{¹H} (in case of selenated and tellurated species, respectively) NMR spectra. Their complexation with Pd(II), Pt(II), Hg(II) and (*p*-cymene)Ru(II) has been explored. The single-crystal structures of ligands L¹, L³ and L⁶ and complexes of Pd(II) with L¹, L², L³ and L⁵ have been determined. The geometry of Pd is close to square planar in all the complexes and the ligands coordinate in a uni-negative tridentate mode. The Pd–N bond lengths are in the range 1.996(7)–2.019(5) Å. The Pd–Se bond distance is 2.3600(5) Å whereas Pd–Te is 2.5025(7) Å. The Pd(II) complexes of L¹–L⁵ have been found promising as homogeneous catalyst for Heck and Suzuki reactions. The yields obtained were up to 85%.

© 2008 Elsevier B.V. All rights reserved.

1. Introduction

1'-Hydroxy-2'-acetonaphthone (HAN) is an important molecule. It has been studied as a proton transfer prototype molecule in gas, solution and nanocavities. The internal hydrogen bonding photoreaction in this molecule leads to keto type structure, and following its formation, an internal twisting motion gives birth to keto rotamers [1]. Its skeleton is very photostable and used for polymer photoprotection [2]. It has also been used for preparing photosensitive ZrO₂ films [3]. Its Schiff bases with diamines and amine having an arm of pyrrolidine have been synthesized [4–6]. Their dioxovanadium(V) complexes have also been synthesized, structurally characterized and found promising for several catalytic oxidation reactions. To the best of our knowledge no Schiff base of HAN having chalcogen functionalities has been studied so far. The presence of chalcogen may tune the catalytic activity of its complex in a new direction. Therefore first exam-

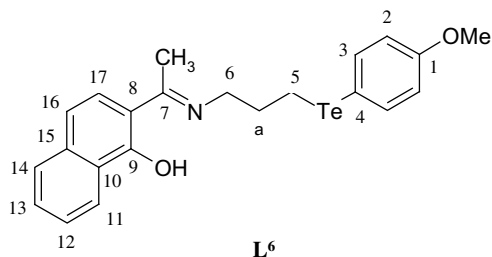
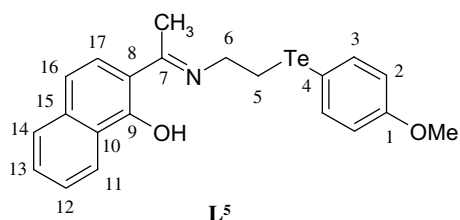
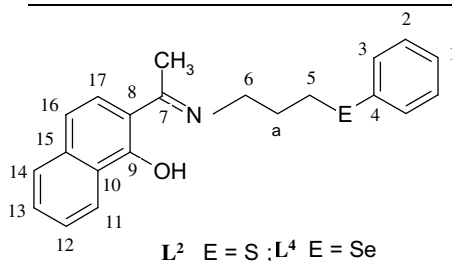
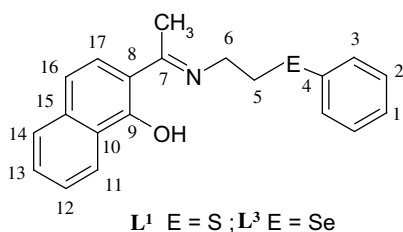
ples of Schiff bases of 1'-hydroxy-2'-acetonaphthone containing chalcogen functionalities (L¹–L⁶) are reported here. Their complexes having stoichiometries [PdCl(L–H)] (L = L¹–L⁶; L–H = deprotonated ligand.), [PtCl(L³–H/L⁵–H)], [PtCl₂(L⁴/L⁶)₂], [(*p*-cymene)RuCl(L⁵/L⁶)]Cl and [HgBr₂(L⁵/L⁶)₂] have been synthesized. The ligands and their complexes have been characterized using multinuclei NMR, IR and mass spectral data and single-crystal structures (in case of some ligands and palladium(II) complexes). These results and potential of some of Pd(II) complexes as homogeneous catalysts for Heck and Suzuki reactions are the subject of the present paper.

2. Experimental

The C and H analyses were carried out with a Perkin–Elmer 2400 Series II C, H, N analyzer. The ¹H, ¹³C{¹H}, ⁷⁷Se{¹H} NMR and ¹²⁵Te{¹H} NMR spectra were recorded on a Bruker Spectrospin DPX-300 NMR spectrometer at 300.13, 75.47, 57.24 and 94.69 MHz, respectively. Mass spectra (ion spray) were recorded on Hybrid Quadrupole-TOF LC/MS/MS mass spectrometer (QSTAR XL System), Model 1011273/A, AB Sciex Instruments (Applied Biosystems, Canada).

* Corresponding author. Tel.: +91 11 26591379; fax: +91 11 26581102.

E-mail addresses: aksingh@chemistry.iitd.ac.in, ajai57@hotmail.com (A.K. Singh).



IR spectra in the range 4000–250 cm⁻¹ were recorded on a Nicolet Protège 460 FT-IR spectrometer as KBr pellets. The melting points determined in open capillary are reported as such. The conductivity measurements were carried out in CH₃CN (concentration ca. 1 mM) using ORION conductivity meter model 162.

Single-crystal diffraction studies were carried out with a Bruker AXS SMART Apex CCD diffractometer using Mo K α (0.71073 Å) radiations at 298(2) K The software S_{AD}ABS was used for absorption correction (if needed) and SHELXTL for space group, structure determination and refinements [7,8]. All non-hydrogen atoms were refined anisotropically. Hydrogen atoms were included in idealized positions with isotropic thermal parameters set at 1.2 times that of the carbon atom to which they are attached. The least-squares refinement cycles on F^2 were performed until the model converged. The precursor chalcogenated amines PhS(CH₂)₂NH₂, PhS(CH₂)₃NH₂, PhSe(CH₂)₂NH₂, PhSe(CH₂)₃NH₂, ArTe(CH₂)₂NH₂ and ArTe(CH₂)₃NH₂ [Ar = 4-CH₃O-C₆H₄] were synthesized by the literature methods [9–11].

2.1. Synthesis of L¹–L⁶

2-(Phenylsulphonyl)ethylamine (0.765 g, 5.0 mmol)/2-(phenylseleno)ethylamine (1.00 g, 5.0 mmol)/2-(4-methoxyphenyltelluro)ethylamine (1.39 g, 5.0 mmol)/3-(phenylsulphonyl)propylamine (0.835 g, 5.0 mmol)/3-(phenylseleno)propylamine (1.07 g, 5.0 mmol) /3-(4-methoxyphenyl telluro)propylamine (1.46 g, 5.0 mmol) was stirred in dry ethanol (20 mL) at room temperature for 0.5 h. HAN (0.93 g, 5.0 mmol), dissolved in dry ethanol (20 mL), was added dropwise with stirring. The mixture was stirred further at room temperature for 2 h. The solvent was evaporated off on a rotary evaporator. The L¹–L⁴ and L⁶ were obtained as a yellow precipitate and L⁵ as yellow coloured highly viscous liquid. The precipitates were recrystallized with chloroform–hexane mixture (1:1). It gave yellow coloured single crystals in the case of L¹, L³ and L⁶. The L⁵ was purified by washing it with 10 mL hexane–chloroform mixture (3:1). All ligands L¹–L⁶ were finally dried in vacuo.

2.1.1. Ligand L¹

Yield 1.446 g (~90%); m.p. 62 °C. $A_M = 0.6 \text{ cm}^2 \text{ mol}^{-1} \text{ ohm}^{-1}$. Anal. Calc. for C₂₀H₁₉NOS: C, 74.66; H, 5.91; N, 4.35. Found: C, 74.82; H, 5.89; N, 4.41%. NMR (¹H, CDCl₃, 25 °C, vs. TMS): δ

2.22 (s, 3H, CH₃), 3.18 (t, $J = 7.2 \text{ Hz}$, 6.9 Hz, 2H, H₅), 3.59–3.63 (m, 2H, H₆), 6.78 (d, $J = 9.3 \text{ Hz}$, 1H, H₁₆), 7.19–7.24 (m, 2H, H₁, H₁₇), 7.28 (t, $J = 7.4 \text{ Hz}$, 2H, H₂), 7.37–7.41 (m, 3H, H₃ and H₁₂), 7.49 (t, $J = 6.9 \text{ Hz}$, 1H, H₁₃), 7.57 (d, $J = 7.8 \text{ Hz}$, 1H, H₁₄) 8.50 (d, $J = 8.1 \text{ Hz}$, 1H, H₁₁), 16.38 (bs, 1H, OH); (¹³C{¹H}), CDCl₃, 25 °C, vs. TMS): δ 14.08 (CH₃), 33.62 (C₅), 44.24 (C₆), 108.57 (C₈), 113.45 (C₁₆), 124.66 (C₁₇ and C₁₂), 125.38 (C₁₁), 126.85 (C₁₄), 126.87 (C₁), 129.08 (C₂), 129.52 (C₁₃), 130.17 (C₁₀), 130.25 (C₃), 134.26 (C₄), 137.07 (C₁₅), 170.93 (C₉), 175.12 (C₇); HRMS (ESI+) calc. for KC₂₀H₁₉NOS (M+K)⁺ 360.0824, found m/z 360.0820 (Δ 1.2334 ppm). IR(KBr, cm⁻¹): 3423, 1612, 785.

2.1.2. Ligand L²

Yield 1.543 g (~92%); m.p. 64 °C. $A_M = 0.8 \text{ cm}^2 \text{ mol}^{-1} \text{ ohm}^{-1}$. Anal. Calc. for C₂₁H₂₁NOS: C, 75.12; H, 6.26; N, 4.17. Found: C, 75.19; H, 6.23; N, 4.13%. NMR (¹H, CDCl₃, 25 °C, vs. TMS): δ 2.01 (quintet, $J = 6.6 \text{ Hz}$, 2H, Ha), 2.24 (s, 3H, CH₃), 3.01 (t, $J = 6.6 \text{ Hz}$, 2H, H₅), 3.50–3.52 (m, 2H, H₆), 6.76 (d, $J = 9.3 \text{ Hz}$, 1H, H₁₆), 7.13–7.27 (m, 4H, H₁, H₂, H₁₇), 7.32 (d, $J = 7.5 \text{ Hz}$, 2H, H₃), 7.39 (t, $J = 7.2 \text{ Hz}$, 1H, H₁₂), 7.49 (t, $J = 7.5 \text{ Hz}$, 1H, H₁₃), 7.57 (d, $J = 7.8 \text{ Hz}$, 1H, H₁₄) 8.50 (d, $J = 8.1 \text{ Hz}$, 1H, H₁₁), 16.22 (bs, 1H, OH); (¹³C{¹H}), CDCl₃, 25 °C, vs. TMS): δ 13.94 (CH₃), 28.55 (Ca) 30.59 (C₅), 43.07 (C₆), 108.26 (C₈), 112.99 (C₁₆), 124.55 (C₁₇), 124.71 (C₁₂), 125.32 (C₁₁), 126.16 (C₁), 126.86 (C₁₄), 128.88 (C₂), 129.31 (C₃), 129.46 (C₁₃), 130.43 (C₁₀), 135.21 (C₄), 137.11 (C₁₅), 171.00 (C₉), 175.70 (C₇); IR(KBr, cm⁻¹): 3421, 1612, 786.

2.1.3. Ligand L³

Yield 1.694 g (~92%); m.p. 78 °C. $A_M = 0.8 \text{ cm}^2 \text{ mol}^{-1} \text{ ohm}^{-1}$. Anal. Calc. for C₂₀H₁₉NOSe: C, 65.16; H, 5.15; N, 3.80. Found: C, 65.08; H, 5.17; N, 3.89%. NMR (¹H, CDCl₃, 25 °C, vs. TMS): δ 2.37 (s, 3H, CH₃), 3.19 (t, $J = 7.2 \text{ Hz}$, 7.5 Hz, 2H, H₅), 3.78–3.84 (m, 2H, H₆), 6.82 (d, $J = 9.3 \text{ Hz}$, 1H, H₁₆), 7.26–7.29 (m, 4H, H₁, H₂, H₁₇), 7.41 (t, $J = 6.6 \text{ Hz}$, 8.1 Hz, 1H, H₁₂), 7.50–7.61 (m, 4H, H₃, H₁₃, H₁₄), 8.50 (d, $J = 8.1 \text{ Hz}$, 1H, H₁₁), 16.43 (bs, 1H, OH); (¹³C{¹H}), CDCl₃, 25 °C, vs. TMS): δ 14.11 (CH₃), 26.53 (C₅), 45.21 (C₆), 108.59 (C₈), 113.53 (C₁₆), 124.67 (C₁₇), 124.72 (C₁₂), 125.47 (C₁₁), 126.92 (C₁₄), 127.61 (C₁), 128.39 (C₄), 129.27 (C₂), 129.58 (C₁₃), 130.31 (C₁₀), 133.41 (C₃), 137.14 (C₁₅), 170.62 (C₉), 175.35 (C₇); (⁷⁷Se{¹H}), CDCl₃, 25 °C, vs. Me₂Se): δ 287.7. HRMS (ESI+) calc. for HC₂₀H₁₉NOSe (M+H)⁺ 370.0710, found m/z 370.0709 (Δ 0.2971 ppm). IR(KBr, cm⁻¹): 3438, 1612, 472, 740.

2.1.4. Ligand **L**⁴

Yield 1.739 g (~91%); m.p. 82 °C. $\Lambda_M = 0.7 \text{ cm}^2 \text{ mol}^{-1} \text{ ohm}^{-1}$. Anal. Calc. for $\text{C}_{21}\text{H}_{21}\text{NOSe}$: C, 65.92; H, 5.49; N, 3.66. Found: C, 65.90; H, 5.47; N, 3.69%. NMR (¹H, CDCl₃, 25 °C, vs. TMS): δ 1.97 (quintet, $J = 7.2 \text{ Hz}$, 2H, Ha), 2.01 (s, 3H, CH₃), 2.90 (t, $J = 7.2 \text{ Hz}$, 2H, H₅), 3.25 (t, $J = 6.9 \text{ Hz}$, 2H, H₆), 6.74 (d, $J = 9.3 \text{ Hz}$, 1H, H₁₆), 7.13 (d, $J = 9.0 \text{ Hz}$, 1H, H₁₇), 7.18–7.21 (m, 3H, H₁ + H₂), 7.38–7.56 (m, 4H, H₃, H₁₂, H₁₃), 7.57 (d, $J = 7.2 \text{ Hz}$, 1H, H₁₄), 8.57 (d, $J = 8.1 \text{ Hz}$, 1H, H₁₁), 16.09 (bs, 1H, OH); (¹³C{¹H}), CDCl₃, 25 °C, vs. TMS): δ 13.46 (CH₃), 23.92 (C₅), 29.09 (Ca), 43.65 (C₆), 107.91 (C₈), 112.41 (C₁₆), 124.14 (C₁₇), 124.60 (C₁₂), 125.04 (C₁₁), 126.56 (C₁₄ as well as C₁), 128.72 (C₂), 129.00 (C₄), 129.09 (C₁₃), 130.16 (C₁₀), 132.07 (C₃), 136.81 (C₁₅), 170.68 (C₉), 175.23 (C₇); (⁷⁷Se{¹H}), CDCl₃, 25 °C, vs. Me₂Se): δ 288.8. IR(KBr, cm⁻¹): 3435, 1612, 740, 472.

2.1.5. Ligand **L**⁵

Yield 2.1232 g (~95%); $\Lambda_M = 0.9 \text{ cm}^2 \text{ mol}^{-1} \text{ ohm}^{-1}$. Anal. Calc. for $\text{C}_{21}\text{H}_{21}\text{NO}_2\text{Te}$: C, 56.37; H, 4.69; N, 3.13. Found: C, 56.24; H, 4.72; N, 3.09%. NMR (¹H, CDCl₃, 25 °C, vs. TMS): δ 2.25 (s, 3H, CH₃), 3.00 (t, $J = 8.1 \text{ Hz}$, 2H, H₅), 3.72 (s, 3H, OMe), 3.79 (m, 2H, H₆), 6.71 (d, $J = 8.7 \text{ Hz}$, 2H, H₂), 6.77 (d, $J = 9.3 \text{ Hz}$, 1H, H₁₆), 7.21 (d, $J = 9.0 \text{ Hz}$, 1H, H₁₇), 7.39 (t, $J = 6.9 \text{ Hz}$, 1H, H₁₂), 7.50 (t, $J = 6.6 \text{ Hz}$, 1H, H₁₃), 7.57 (d, $J = 8.4 \text{ Hz}$, 1H, H₁₄), 7.70 (d, $J = 8.7 \text{ Hz}$, 2H, H₃), 8.48 (d, $J = 8.1 \text{ Hz}$, 1H, H₁₁), 16.19 (bs, 1H, OH); (¹³C{¹H}), CDCl₃, 25 °C, vs. TMS): δ 6.23 (C₅), 13.97 (CH₃), 46.91 (C₆), 55.00 (OCH₃), 99.22 (C₄), 108.37 (C₈), 113.29 (C₁₆), 115.28 (C₂), 124.65 (C₁₇), 124.68 (C₁₂), 125.49 (C₁₁), 126.87 (C₁₄), 129.56 (C₁₃), 130.46 (C₁₀), 137.17 (C₁₅), 141.46 (C₃), 160.01 (C₁), 170.17 (C₉), 175.79 (C₇); (¹²⁵Te{¹H}), CDCl₃, 25 °C, vs. Me₂Te): δ 466.1. IR(KBr, cm⁻¹): 3438, 1613, 518.

2.1.6. Ligand **L**⁶

Yield 2.189 g (~95%); $\Lambda_M = 0.9 \text{ cm}^2 \text{ mol}^{-1} \text{ ohm}^{-1}$. Anal. Calc. for $\text{C}_{22}\text{H}_{23}\text{NO}_2\text{Te}$: C, 57.26; H, 4.99; N, 3.04. Found: C, 57.24; H, 4.91; N, 3.09%. NMR (¹H, CDCl₃, 25 °C, vs. TMS): δ 2.13 (quintet, $J = 7.2 \text{ Hz}$, 2H, Ha), 2.24 (s, 3H, CH₃), 2.88 (t, $J = 7.5 \text{ Hz}$, 2H, H₅), 3.45 (m, 2H, H₆), 3.69 (s, 3H, OMe), 6.68 (d, $J = 9.0 \text{ Hz}$, 2H, H₂), 6.75 (d, $J = 9.0 \text{ Hz}$, 1H, H₁₆), 7.20 (d, $J = 9.3 \text{ Hz}$, 1H, H₁₇), 7.39 (t, $J = 7.5 \text{ Hz}$, 1H, H₁₂), 7.49 (t, $J = 6.9 \text{ Hz}$, 1H, H₁₃), 7.56 (d, $J = 7.8 \text{ Hz}$, 1H, H₁₄), 7.64 (d, $J = 8.4 \text{ Hz}$, 2H, H₃), 8.49 (d, $J = 8.1 \text{ Hz}$, 1H, H₁₁), 16.12 (bs, 1H, OH); (¹³C{¹H}), CDCl₃, 25 °C, vs. TMS): δ 4.78 (C₅), 14.04 (CH₃), 31.05 (Ca), 46.09 (C₆), 54.95 (OCH₃), 99.73 (C₄), 108.23 (C₈), 112.92 (C₁₆), 115.14 (C₂), 124.53 (C₁₇), 124.70 (C₁₂), 125.38 (C₁₁), 126.85 (C₁₄), 129.46 (C₁₃), 130.53 (C₁₀), 137.15 (C₁₅), 140.80 (C₃), 159.68 (C₁), 170.83 (C₉), 175.86 (C₇); (¹²⁵Te{¹H}), CDCl₃, 25 °C, vs. Me₂Te): δ 460.3. HRMS (ESI⁺) calc. for $\text{HC}_{22}\text{H}_{23}\text{NO}_2\text{Te}$ (M+H)⁺ 464.0869, found m/z 464.0862 (Δ 1.5800 ppm). IR(KBr, cm⁻¹): 1645, 504, 292.

2.2. Synthesis of [PdCl(L-H)] and [PtCl(L-H)]

$\text{Na}_2[\text{PdCl}_4]$ (0.294 g, 1 mmol) was dissolved in water (5 mL) and mixed with the solution of 1 mmol of **L**¹ (0.321 g)/**L**² (0.335 g)/**L**³ (0.368 g)/**L**⁴ (0.382 g)/**L**⁵ (0.447 g)/**L**⁶ (0.461 g) in acetone (10 mL). Similarly $\text{K}_2[\text{PtCl}_4]$ (0.415 g, 1 mmol) was mixed with the solutions of **L**³ and **L**⁵. The mixture was vigorously stirred for 0.5 h. An orange precipitate was immediately obtained, which was filtered, washed with hexane (10 mL) and dried in vacuo. Its recrystallization with chloroform–hexane (60:40) mixture gave red coloured single crystals of [PdCl(L-H)] (**L** = **L**¹–**L**³, **L**⁵).

2.2.1. [PdCl(L¹-H)] (**1**)

Yield 0.360 g (~78%); m.p. 160 °C. $\Lambda_M = 5.0 \text{ cm}^2 \text{ mol}^{-1} \text{ ohm}^{-1}$. Anal. Calc. for $\text{C}_{20}\text{H}_{18}\text{NOSPdCl}$: C, 51.92; H, 3.89; N, 3.03. Found:

C, 51.87; H, 3.91; N, 3.09%. NMR (¹H, CDCl₃, 25 °C, vs. TMS): δ 2.29 (s, 3H, CH₃), 2.69–2.73 (m, 1H, H₅), 3.49–3.89 (m, 3H, H₅ + H₆), 6.96 (d, $^3J = 9.0 \text{ Hz}$, 1H, H₁₆), 7.27 (d, $^3J = 9.0 \text{ Hz}$, 1H, H₁₇), 7.40–7.46 (m, 4H, H₁, H₂ and H₁₂), 7.55 (t, $^3J = 7.2 \text{ Hz}$, 1H, H₁₃), 7.63 (d, $^3J = 7.8 \text{ Hz}$, 1H, H₁₄), 8.17–8.20 (m, 2H, H₃), 8.73 (d, $^3J = 8.1 \text{ Hz}$, 1H, H₁₁), (¹³C{¹H}), CDCl₃, 25 °C, vs. TMS): δ 19.61 (CH₃), 41.36 (C₅), 58.84 (C₆), 115.17 (C₈), 115.66 (C₁₆), 125.15 (C₁₂), 126.36 (C₁₄), 126.56 (C₁₁), 127.17 (C₁₇), 128.16 (C₁₀), 128.57 (C₄), 129.15 (C₁₃), 129.77 (C₂), 130.60 (C₁), 133.02 (C₃), 136.09 (C₁₅), 162.59 (C₉), 167.00 (C₇); IR(KBr, cm⁻¹): 1596, 745.

2.2.2. [PdCl(L²-H)] (**2**)

Yield 0.400 g (~84%); m.p. 162 °C. $\Lambda_M = 6.0 \text{ cm}^2 \text{ mol}^{-1} \text{ ohm}^{-1}$. Anal. Calc. for $\text{C}_{21}\text{H}_{20}\text{NOSPdCl}$: C, 52.91; H, 4.20; N, 2.94. Found: C, 52.87; H, 4.23; N, 2.90%. NMR (¹H, CDCl₃, 25 °C, vs. TMS): δ 2.16–2.22 (m, 2H, Ha), 2.44 (s, 3 H, CH₃), 2.99 (m, 2H, H₅), 3.70–3.74 (m, 2H, H₆), 7.03 (d, $^3J = 9.0 \text{ Hz}$, 1H, H₁₆), 7.33 (d, $^3J = 9.0 \text{ Hz}$, 1H, H₁₇), 7.39–7.43 (m, 4H, H₁, H₂ and H₁₂), 7.51 (t, $^3J = 6.9 \text{ Hz}$, 1H, H₁₃), 7.63 (d, $^3J = 8.1 \text{ Hz}$, 1H, H₁₄), 8.06–8.09 (m, 2H, H₃), 8.66 (d, $^3J = 8.1 \text{ Hz}$, 1H, H₁₁), (¹³C{¹H}), CDCl₃, 25 °C, vs. TMS): δ 19.64 (CH₃), 25.77 (Ca), 34.53 (C₅), 51.58 (C₆), 115.70 (C₈ as well as C₁₆), 121.71 (C₄), 125.37 (C₁₇), 125.80 (C₁₄), 126.60 (C₁₂), 127.03 (C₁₁), 129.11 (C₁₃), 129.68 (C₂), 129.86 (C₁₀), 130.11 (C₁), 132.40 (C₃), 136.52 (C₁₅), 162.54 (C₉), 167.30 (C₇); IR(KBr, cm⁻¹): 1598, 748.

2.2.3. [PdCl(L³-H)] (**3**)

Yield ~0.397 g (~78%); m.p. 142 °C. $\Lambda_M = 5.0 \text{ cm}^2 \text{ mol}^{-1} \text{ ohm}^{-1}$. Anal. Calc. for $\text{C}_{20}\text{H}_{18}\text{NOSPdCl}$: C, 47.14; H, 3.53; N, 2.74. Found: C, 47.09; H, 3.49; N, 2.81%. NMR (¹H, CDCl₃, 25 °C, vs. TMS): δ 2.07 (s, 3H, CH₃), 2.66–2.71 (m, 1H, H₅), 3.54–3.61 (m, 2H, H₅ + H₆), 4.15–4.20 (m, 1H, H₆), 6.99 (d, $^3J = 9.0 \text{ Hz}$, 1H, H₁₆), 7.22 (d, $^3J = 9.3 \text{ Hz}$, 1H, H₁₇), 7.41–7.45 (m, 4H, H₁, H₂, H₁₂), 7.54 (t, $^3J = 6.6 \text{ Hz}$, 6.9 Hz, 1H, H₁₃), 7.64 (d, $^3J = 7.5 \text{ Hz}$, 1H, H₁₄), 8.18–8.22 (m, 2H, H₃), 8.74 (d, $^3J = 8.1 \text{ Hz}$, 1H, H₁₁), (¹³C{¹H}), CDCl₃, 25 °C, vs. TMS): δ 19.66 (CH₃), 32.71 (C₅), 60.29 (C₆), 115.27 (C₁₆), 115.78 (C₈), 125.10 (C₁₂), 125.54 (C₄), 126.36 (C₁₄), 127.00 (C₁₁), 127.18 (C₁₇), 128.11 (C₁₀), 129.10 (C₁₃), 129.93 (C₂), 130.16 (C₁), 133.64 (C₃), 136.06 (C₁₅), 162.85 (C₉), 167.26 (C₇); (⁷⁷Se{¹H}), CDCl₃, 25 °C, vs. Me₂Se): δ 445.7. IR(KBr, cm⁻¹): 1571, 468, 742.

2.2.4. [PtCl(L³-H)] (**4**)

Yield ~0.531 g (~89%); m.p. 168 °C; $\Lambda_M = 8.0 \text{ cm}^2 \text{ mol}^{-1} \text{ ohm}^{-1}$. Anal. Calc. for $\text{C}_{20}\text{H}_{18}\text{NOSPtCl}$: C, 40.15; H, 3.01; N, 2.34. Found: C, 40.09; H, 3.04; N, 2.31%. NMR (¹H, CDCl₃, 25 °C, vs. TMS): δ 2.41 (s, 3H, CH₃), 3.22–3.28 (m, 1H, H₅), 3.77–3.96 (m, 3H, H₅ + H₆), 6.99 (d, $^3J = 9.3 \text{ Hz}$, 1H, H₁₆), 7.31 (d, $^3J = 9.3 \text{ Hz}$, 1H, H₁₇), 7.34–7.44 (m, 4H, H₁, H₂, H₁₂), 7.52 (t, $^3J = 6.9 \text{ Hz}$, 1H, H₁₃), 7.64 (d, $^3J = 6.9 \text{ Hz}$, 1H, H₁₄), 8.07–8.09 (m, 2H, H₃), 8.78 (d, $^3J = 8.1 \text{ Hz}$, 1H, H₁₁), (¹³C{¹H}), CDCl₃, 25 °C, vs. TMS): δ 20.54 (CH₃), 34.22 (C₅), 61.88 (C₆), 114.16 (C₈), 115.83 (C₁₆), 125.32 (C₁₂), 125.92 (C₄), 126.76 (C₁₄), 127.43 (C₁₁), 127.58 (C₁₇), 128.51 (C₁₀), 129.54 (C₁₃), 129.97 (C₂), 130.46 (C₁), 133.84 (C₃), 136.86 (C₁₅), 162.98 (C₉), 163.46 (C₇); (⁷⁷Se{¹H}), CDCl₃, 25 °C, vs. Me₂Se): δ 388.6. IR(KBr, cm⁻¹): 1582, 468, 740.

2.2.5. [PdCl(L⁴-H)] (**5**)

Yield ~0.455 g (~87%); m.p. 148 °C. $\Lambda_M = 7.0 \text{ cm}^2 \text{ mol}^{-1} \text{ ohm}^{-1}$. Anal. Calc. for $\text{C}_{21}\text{H}_{20}\text{NOSPdCl}$: C, 48.17; H, 3.82; N, 2.68. Found: C, 48.13; H, 3.79; N, 2.63%. NMR (¹H, CDCl₃, 25 °C, vs. TMS): δ 1.97–2.06 (m, 1H, Ha), 2.27–2.37 (m, 4H, CH₃ + Ha), 2.75 (t of d, $^2J = 12.9 \text{ Hz}$, $^3J = 5.4 \text{ Hz}$, 1H, H₅), 3.07 (d of t, $^3J = 9.6 \text{ Hz}$, $^2J = 4.5 \text{ Hz}$, 1H, H₅), 3.51–3.65 (m, 2H, H₆), 6.95 (d, $^3J = 9.0 \text{ Hz}$, 1H, H₁₆), 7.27 (d, $^3J = 9.0 \text{ Hz}$, 1H, H₁₇), 7.33–7.41 (m, 4H, H₁, H₂, H₁₂), 7.49 (t, $^3J = 7.8 \text{ Hz}$, 1H, H₁₃), 7.62 (d, $^3J = 8.1 \text{ Hz}$, 1H, H₁₄), 8.06 (d, $^3J = 7.8 \text{ Hz}$,

2H, H₃), 8.64 (d, ³J = 8.1 Hz, 1H, H₁₁), (¹³C{¹H}, CDCl₃, 25 °C, vs. TMS): δ 19.35 (CH₃), 26.23 (Ca), 29.48 (C₅), 53.03 (C₆), 115.11 (C₁₆), 121.96 (C₈), 125.04 (C₁₂), 126.37 (C₁₇), 126.63 (C₁₄), 126.88 (C₄ as well as C₁₁), 128.79 (C₁₀), 128.87 (C₁₃), 129.72 (C₂), 129.79 (C₁), 133.37 (C₃), 136.47 (C₁₅), 163.86 (C₉), 167.72 (C₇); (⁷⁷Se{¹H}, CDCl₃, 25 °C, vs. Me₂Se): δ 297.01. IR(KBr, cm⁻¹): 1576, 741, 469.

2.2.6. [PdCl(L⁵-H)] (6)

Yield ~0.564 g (~96%); m.p. 173 °C *A*_M = 9.0 cm² mol⁻¹ ohm⁻¹. Anal. Calc. for C₂₁H₂₀NO₂TePdCl: C, 42.87; H, 3.40; N, 2.38. Found: C, 42.81; H, 3.47; N, 2.31%. NMR (¹H, CDCl₃, 25 °C, vs. TMS): δ 1.86 (s, 3H, CH₃), 2.35 (t of d, ²J = 12 Hz, ³J = 4.8 Hz, 1H, H₅), 3.40 (d of t, ³J = 12 Hz, ³J = 4.8 Hz, 1H, H₅), 3.78 (s, 3H, OCH₃), 3.86 (d of t, ³J = 12.9 Hz, ³J = 3.9 Hz, 1H, H₆), 5.19 (t of d, ²J = 13.2 Hz, ³J = 3.9 Hz, 1H, H₆), 6.84 (d, ³J = 8.4 Hz, 2H, H₂), 6.93 (d, ³J = 9.3 Hz, 1H, H₁₆), 7.11 (d, ³J = 9.0 Hz, 1H, H₁₇), 7.40 (t, ³J = 7.2 Hz, 1H, H₁₂), 7.52 (t, ³J = 7.2 Hz, 1H, H₁₃), 7.64 (d, ³J = 7.8 Hz, 1H, H₁₄), 7.98 (d, ³J = 8.7 Hz, 2H, H₃), 8.71 (d, ³J = 8.1 Hz, 1H, H₁₁), (¹³C{¹H}, CDCl₃, 25 °C, vs. TMS): δ 14.65 (C₅), 19.72 (CH₃), 55.28 (OCH₃), 63.09 (C₆), 104.36 (C₄), 114.22 (C₁₆), 115.66 (C₂), 116.63 (C₈), 124.67 (C₁₂), 126.35 (C₁₄), 126.70 (C₁₁), 128.13 (C₁₀), 128.16 (C₁₇), 128.78 (C₁₃), 135.98 (C₁₅), 138.69 (C₃), 161.10 (C₁), 162.77 (C₉), 167.98 (C₇); (¹²⁵Te{¹H}, CDCl₃, 25 °C, vs. Me₂Te): δ 764.1. IR(KBr, cm⁻¹): 1596, 515, 292.

2.2.7. [PtCl(L⁵-H)] (7)

Yield ~0.6020 g (~89%); m.p. 178 °C *A*_M = 10.0 cm² mol⁻¹ ohm⁻¹. Anal. Calc. for C₂₁H₂₀NO₂TePtCl: C, 37.25; H, 2.96; N, 2.07. Found: C, 37.19; H, 2.91; N, 2.09%. NMR (¹H, CDCl₃, 25 °C, vs. TMS): δ 1.69 (s, 3H, CH₃), 2.11–2.15 (m, 1H, H₅), 3.36–3.53 (m, 2H, 2H, H₅ + H₆), 3.77 (s, 3H, OCH₃), 4.61–4.65 (m, 1H, H₆), 6.81 (d, ³J = 8.4 Hz, 2H, H₂), 6.99 (d, ³J = 9.0 Hz, 1H, H₁₆), 7.19 (d, ³J = 9.0 Hz, 1H, H₁₇), 7.42 (t, ³J = 6.9 Hz, 1H, H₁₂), 7.57 (t, ³J = 6.9 Hz, 1H, H₁₃), 7.65 (d, ³J = 7.8 Hz, 1H, H₁₄), 7.94 (d, ³J = 8.4 Hz, 2H, H₃), 8.78 (d, ³J = 8.1 Hz, 1H, H₁₁), (¹³C{¹H}, CDCl₃, 25 °C, vs. TMS): δ 15.09 (C₅), 20.74 (CH₃), 55.24 (OCH₃), 63.84 (C₆), 101.12 (C₄), 115.09 (C₁₆ + C₂), 116.31 (C₈), 125.06 (C₁₂), 126.43 (C₁₄), 126.56 (C₁₁), 127.58 (C₁₇), 128.01 (C₁₀), 128.66 (C₁₃), 135.50 (C₁₅), 138.16 (C₃), 160.41 (C₉), 161.17 (C₁), 163.73 (C₇); (¹²⁵Te{¹H}, CDCl₃, 25 °C, vs. Me₂Te) 624.9. IR(KBr, cm⁻¹): 1582, 512, 280.

2.2.8. [PdCl(L⁶-H)] (8)

Yield ~0.536 g (~89%); m.p. 176 °C *A*_M = 10.0 cm² mol⁻¹ ohm⁻¹. Anal. Calc. for C₂₂H₂₂NO₂TePdCl: C, 43.86; H, 3.66; N, 2.33. Found: C, 43.81; H, 3.69; N, 2.24%. NMR (¹H, CDCl₃, 25 °C, vs. TMS): δ 2.02 (m, 1H, Ha), 2.24 (s, 3H, CH₃), 2.39 (m, 1H, Ha), 2.55–2.59 (m, 1H, H₅), 2.84–2.87 (m, 1H, H₅), 3.64–3.66 (m, 2H, H₆), 3.79 (s, 3H, OCH₃), 6.83 (d, ³J = 8.1 Hz, 2H, H₂), 6.92 (d, ³J = 9.0 Hz, 1H, H₁₆), 7.25 (d, ³J = 9.3 Hz, 1H, H₁₇), 7.37 (t, ³J = 7.2 Hz, 1H, H₁₂), 7.48 (t, ³J = 7.8 Hz, 1H, H₁₃), 7.62 (d, ³J = 8.1 Hz, 1H, H₁₄), 8.00 (d, ³J = 8.1 Hz, 2H, H₃), 8.64 (d, ³J = 8.4 Hz, 1H, H₁₁), (¹³C{¹H}, CDCl₃, 25 °C, vs. TMS): δ 15.60 (C₅), 19.20 (CH₃), 26.48 (Ca) 55.31 (OCH₃), 57.56 (C₆), 104.49 (C₄), 114.45 (C₁₆), 115.64 (C₂), 121.95 (C₈), 124.89 (C₁₂), 126.64 (C₁₄), 126.71 (C₁₇), 126.93 (C₁₁), 128.76 (C₁₃), 129.14 (C₁₀), 136.54 (C₁₅), 138.70 (C₃), 161.06 (C₁), 164.17 (C₉), 168.21 (C₇); (¹²⁵Te{¹H}, CDCl₃, 25 °C, vs. Me₂Te): δ 484.75. IR(KBr, cm⁻¹): 1598, 513, 292.

2.3. Synthesis of [PtCl₂(L⁴)₂] (9) and [PtCl₂(L⁶)₂] (10)

K₂[PtCl₄] (0.415 g, 1 mmol) dissolved in water (5 mL) and a solution of 2 mmol of L⁴ (0.764 g)/L⁶ (0.922 g) in acetone (10 mL) were stirred together vigorously. An orange precipitate of **9** or **10** was immediately obtained, which was filtered, washed with hexane (10 mL) and dried in vacuo.

2.3.1. Compound 9

Yield ~0.83 g (~80%); m.p. 156 °C; *A*_M = 6.6 cm² mol⁻¹ ohm⁻¹. Anal. Calc. for C₄₂H₄₂N₂O₂Se₂PtCl₂: C, 48.91; H, 4.08; N, 2.72. Found: C, 49.10; H, 4.05; N, 2.78%. NMR (¹H, CDCl₃, 25 °C, vs. TMS): δ 2.08–2.18 (m, 4H, Ha), 2.38–2.44 (4s, 6H, CH₃), 3.09–3.68 (m, 8H, H₅ + H₆), 6.81–6.86 (m, 2H, H₁₆), 7.22–7.54 (m, 12H, H₁₇ + H₁₃ + H₁₂ + H₁ + H₂), 7.22–7.59 (m, ³J = 7.5 Hz, 2H, H₁₄), 7.88 (m, 4H, H₃), 8.46 (d, ³J = 7.8 Hz, 2H, H₁₁), 16.44 (bs, 2H, OH), (¹³C{¹H}, CDCl₃, 25 °C, vs. TMS): δ 14.41 (CH₃), 27.61 (C₅), 30.70 (Ca), 44.61 (C₆), 108.11 (C₈), 113.79 (C₁₆), 124.62 (C₁₇), 124.89 (C₁₂), 125.42 (C₁₁), 127.06 (C₁₄), 129.68 (C₂), 129.75 (C₁₃), 130.43 (C₁), 130.91 (C₁₀), 132.94, 132.99 (C₃), 133.17 (C₄), 136.87 (C₁₅), 170.63 (C₉), 175.28 (C₇); (⁷⁷Se{¹H}, CDCl₃, 25 °C, vs. Me₂Se): δ 339.02, 340.27. HRMS (ESI+) calc. for C₄₂H₄₂N₂O₂Se₂Pt (M⁺–2Cl) 961.1225, found *m/z* 961.1240 (Δ 1.6075 ppm). IR(KBr, cm⁻¹): 3444, 1595, 795, 742, 690, 467, 338.

2.3.2. Compound 10

Yield ~0.97 g (~82%); m.p. 154 °C *A*_M = 7.2 cm² mol⁻¹ ohm⁻¹. Anal. Calc. for C₄₄H₄₆N₂O₄Te₂PtCl₂: C, 44.45; H, 3.87; N, 2.36. Found: C, 44.76; H, 3.87; N, 2.40. NMR (¹H, CDCl₃, 25 °C, vs. TMS): δ 1.94–1.98 (m, 4H, Ha), 2.28 (s, 3H, CH₃), 2.35 (s, 3H, CH₃), 2.92–3.43 (m, 8H, H₅ + H₆), 3.63, 3.68, 3.73 (s, 6H, OCH₃), 6.461, 6.641 (d, ³J = 8.4 Hz, 4H, H₂), 6.74–6.80 (m, 2H, H₁₆), 7.22–7.59 (m, 12H, H₁₇, H₁₄, H₁₃, H₁₂, H₃), 8.40–8.46 (2 merging d, 2H, H₁₁), 16.03 (bs, 2H, OH), (¹³C{¹H}, CDCl₃, 25 °C, vs. TMS): δ 14.48, 14.68 (CH₃), 16.19, 16.31 (C₅), 28.13, 28.24 (Ca), 45.50 (C₆), 55.08, 55.16 (OCH₃), 101.61, 102.61 (C₄), 108.68, 108.86 (C₈), 113.23, 113.39 (C₁₆), 115.14, 115.25 (C₂), 124.64 (C₁₇), 124.95 (C₁₂), 125.38 (C₁₁), 126.99 (C₁₄), 129.57 (C₁₃), 130.36, 130.40 (C₁₀), 137.21 (C₁₅), 137.42, 137.68 (C₃), 161.15, 161.40 (C₁), 171.67, 171.85 (C₉), 175.22, 175.37 (C₇); (¹²⁵Te{¹H}, CDCl₃, 25 °C, vs. Me₂Te): δ 550.9, 563.1. HRMS (ESI+) calc. for C₄₄H₄₆N₂O₄Te₂PtCl₂ (M⁺) 1191.0607, found *m/z* 1191.0636 (Δ 2.4290 ppm), (M⁺–2Cl) 1121.1230, found *m/z* 1121.1171 (Δ 5.2638 ppm). IR(KBr, cm⁻¹): 3451, 1593, 798, 742, 692, 585, 518, 414, 308.

2.4. Synthesis of [(*p*-cymene)RuCl(L⁵)Cl] (11) [(*p*-cymene)RuCl(L⁶)Cl] (12)

The [RuCl₂(*p*-cymene)]₂ (0.306 g, 0.5 mmol) dissolved in dichloromethane (10 mL) and a solution of 1 mmol of L⁵ (0.447 g), or L⁶ (0.461 g) in dichloromethane (20 mL) were stirred together vigorously for 3 h. The solvent was removed on a rotary evaporator which gave **11** or **12** as an orange coloured solid. It was washed with hexane and dried in vacuo.

2.4.1. Compound 11

Yield ~0.587 g (~78%); m.p. 168 °C *A*_M = 42 cm² mol⁻¹ ohm⁻¹. Anal. Calc. for C₃₁H₃₅NO₂TeRuCl₂: C, 49.39; H, 4.65; N, 1.86. Found: C, 49.31; H, 4.61; N, 1.81%. NMR (¹H, CDCl₃, 25 °C, vs. TMS): δ 1.25–1.29 (m, 6H, CH₃ of *i*-pr), 2.13 (s, 3H, CH₃), 2.33 (s, 3H, CH₃ *p* to *i*-pr), 2.85 (m, 1H, CH of *i*-pr), 3.20–3.26 (m, 1H, H₅), 3.57–3.61 (m, 1H, H₅), 3.72–3.82 (m, 5H, OCH₃ + H₆), 4.88 (d, ³J = 5.4 Hz, 1H, ArH of *p*-cymene), 5.24 (d, ³J = 5.4 Hz, 1H, ArH of *p*-cymene), 5.36 (d, ³J = 5.7 Hz, 1H, ArH of *p*-cymene), 5.45 (d, ³J = 5.4 Hz, 1H, ArH of *p*-cymene), 6.75–6.81 (m, 3H, H₂ + H₁₆), 7.26 (d, ³J = 9.3 Hz, 1H, H₁₇), 7.41 (t, ³J = 7.5 Hz, 1H, H₁₂), 7.52 (t, ³J = 8.1 Hz, 1H, H₁₃), 7.59 (d, ³J = 7.5 Hz, 1H, H₁₄), 7.90 (d, ³J = 8.4 Hz, 2H, H₃), 8.48 (d, ³J = 8.1 Hz, 1H, H₁₁), 16.36 (bs, 1 H, –OH), (¹³C{¹H}, CDCl₃, 25 °C, vs. TMS): δ 14.48 (CH₃), 17.30 (C₅), 18.44 (*p*-cymene CH₃), 22.06 and 22.31 (CH₃ of *i*-pr of *p*-cymene), 30.80 (CH of *i*-pr of *p*-cymene), 43.74 (C₆), 55.09 (OCH₃), 81.09, 81.26, 85.05 and 85.15 (ArC of *p*-cymene *m* and *o* to *i*-pr), 98.41 (ArC of *p*-cymene attached to CH₃), 104.28 (ArC of *p*-cymene attached to *i*-pr), 106.14 (C₄),

108.69 (C₈), 113.34 (C₁₆), 115.32 (C₂), 124.51 (C₁₇), 124.75 (C₁₂), 125.36 (C₁₁), 126.84 (C₁₄), 129.39 (C₁₃), 130.14 (C₁₀), 137.07 (C₁₅), 137.68 (C₃), 161.30 (C₁), 171.31 (C₉), 174.93 (C₇); (¹²⁵Te{¹H}, CDCl₃, 25 °C, vs. Me₂Te): δ 515.33. HRMS (ESI+) calc. for C₃₁H₃₅NO₂TeRuCl (M⁺–Cl) 720.0462, found *m/z* 720.0472 (Δ 1.3764 ppm). IR(KBr, cm⁻¹): 3440, 1604, 1249, 1179, 1026, 825, 761, 705.

2.4.2. Compound **12**

Yield ~0.65 g (~85%); m.p. 131 °C. *A*_M = 54 cm² mol⁻¹ ohm⁻¹. Anal. Calc. for C₃₂H₃₇NO₂TeRuCl₂: C, 50.06; H, 4.82; N, 1.82. Found: C, 49.88; H, 4.87; N, 1.85%. NMR (¹H, CDCl₃, 25 °C, vs. TMS): δ 1.17–1.23 (m, 6H, CH₃ of *i*-pr), 2.05–2.14 (m, 5H, CH₃ + Ha), 2.31 (s, 3H, CH₃ *p* to *i*-pr), 2.74–2.83 (multiplet, 1H, CH of *i*-pr), 3.10 (m, 1H, H₅), 3.23 (m, 1H, H₅), 3.46–3.48 (m, 2H, H₆), 3.79 (s, 3H, OCH₃), 4.97 (d, ³*J* = 5.1 Hz, 1H, ArH of *p*-cymene), 5.20 (d, ³*J* = 5.1 Hz, 1H, ArH of *p*-cymene), 5.33 (d, ³*J* = 5.4 Hz, 1H, ArH of *p*-cymene), 5.43 (d, ³*J* = 5.4 Hz, 1H, ArH of *p*-cymene), 6.77 (d, ³*J* = 9.0 Hz, 1H, H₁₆), 6.87 (d, ³*J* = 8.4 Hz, 2H, H₂), 7.24 (d, ³*J* = 9.0 Hz, 1H, H₁₇), 7.36 (t, ³*J* = 6.9 Hz, 1H, H₁₂), 7.49 (t, ³*J* = 7.5 Hz, 1H, H₁₃), 7.57 (d, ³*J* = 7.8 Hz, 1H, H₁₄), 7.84 (d, ³*J* = 8.4 Hz, 2H, H₃), 8.45 (d, ³*J* = 8.1 Hz, 1H, H₁₁), 16.18 (bs, 1H, –OH); (¹³C{¹H}, CDCl₃, 25 °C, vs. TMS): δ 14.20 (CH₃), 14.72 (C₅), 18.31 (*p*-cymene CH₃), 21.79 and 22.79 (CH₃ of *i*-pr of *p*-cymene), 28.62 (Ca), 30.65 (CH of *i*-pr of *p*-cymene), 45.76 (C₆), 55.15 (OCH₃), 80.96, 81.48, 84.65 and 85.23 (ArC of *p*-cymene *m* and *o* to *i*-pr), 97.54 (ArC of *p*-cymene attached to CH₃), 104.24 (ArC of *p*-cymene attached to *i*-pr), 106.12 (C₄), 108.34 (C₈), 113.04 (C₁₆), 115.50 (C₂), 124.46 (C₁₇), 124.73 (C₁₂), 125.26 (C₁₁), 126.84 (C₁₄), 129.40 (C₁₃), 130.39 (C₁₀), 137.04 (C₃), 137.11 (C₁₅), 161.27 (C₁), 171.05 (C₉), 175.59 (C₇); (¹²⁵Te{¹H}, CDCl₃, 25 °C, vs. Me₂Te): δ 535.8 ppm. HRMS (ESI+) calc. for C₃₂H₃₇NO₂TeRuCl (M⁺–Cl) 734.0619, found *m/z* 734.0593 (Δ 3.4861 ppm) IR(KBr, cm⁻¹): 3427, 1591, 1456, 1247, 1179, 1023, 795, 744, 691, 586, 518, 414, 283.

2.5. Synthesis of [HgBr₂(L⁵)₂] (**13**) and [HgBr₂(L⁶)₂] (**14**)

The HgBr₂ (0.360 g, 1.0 mmol) was dissolved in 5 mL of acetone. The solution of L⁵ (0.894 g, 2.0 mmol)/L⁶ (0.922 g, 2.0 mmol) in 10 mL of chloroform was added to it with stirring. The mixture was stirred further for 3 h. The solvent was evaporated off to dryness on a rotary evaporator. The resulting residue was washed with acetone, redissolved in minimum amount of chloroform and mixed with hexane. The resulting precipitate of **13** or **14** was filtered, washed with hexane (10 mL) and dried in vacuo.

2.5.1. Compound **13**

Yield ~0.953 g (~76%); m.p. 161 °C. *A*_M = 10.0 cm² mol⁻¹ ohm⁻¹. Anal. Calc. for C₄₂H₄₂N₂O₄Te₂HgBr₂: C, 40.18; H, 3.35; N, 2.23%. Found: C, 40.13; H, 3.39; N, 2.28%. NMR (¹H, CDCl₃, 25 °C, vs. TMS): δ 2.30 (s, 6H, CH₃), 3.50 (t, ³*J* = 7.2 Hz, 4H, H₅), 3.65 (s, 6H, OMe), 4.00 (t, ³*J* = 6.9 Hz, 4H, H₆), 6.71 (d, ³*J* = 8.7 Hz, 4H, H₂), 6.82 (d, ³*J* = 9.0 Hz, 2H, H₁₆), 7.21 (d, ³*J* = 9.3 Hz, 2H, H₁₇), 7.36 (t, ³*J* = 6.9 Hz, 2H, H₁₂), 7.49 (t, ³*J* = 7.8 Hz, 2H, H₁₃), 7.57 (d, ³*J* = 7.8 Hz, 2H, H₁₄), 7.71 (d, ³*J* = 8.7 Hz, 4H, H₃) 8.38 (d, ³*J* = 8.1 Hz, 2H, H₁₁), 16.21 (bs, 2H, OH); (¹³C{¹H}, CDCl₃, 25 °C, vs. TMS): δ 14.87 (CH₃), 20.60 (C₅), 44.85 (C₆), 55.17 (OCH₃), 101.73 (C₄) 109.21 (C₈), 114.07 (C₁₆), 116.05 (C₂), 124.85 (C₁₇ + C₁₂), 125.35 (C₁₁), 127.01 (C₁₄), 129.55 (C₁₃) 129.70 (C₁₀), 137.05 (C₁₅), 139.58 (C₃), 161.28 (C₁), 171.80 (C₉), 173.78 (C₇); (¹²⁵Te{¹H}, CDCl₃, 25 °C, vs. Me₂Te): δ 362.6. HRMS (ESI+) calc. for C₄₂H₄₂N₂O₄Te₂HgBr (M⁺–Br) 1179.0159, found *m/z* 1179.0170 (Δ 0.9463 ppm). IR(KBr, cm⁻¹): 3412, 1589, 1250, 1179, 1024, 796, 748, 689, 587, 515, 422, 321.

2.5.2. Compound **14**

Yield ~1.064 g (~83%); m.p. 170 °C. *A*_M = 10.0 cm² mol⁻¹ ohm⁻¹. Anal. Calc. for C₄₄H₄₆N₂O₄Te₂HgBr₂: C, 41.17; H, 3.59; N, 2.18. Found: C, 41.21; H, 3.51; N, 2.16%. NMR (¹H, CDCl₃, 25 °C, vs. TMS): δ 2.19 (Quintet, *J* = 6.9 Hz, 4H, Ha), 2.25 (s, 6H, CH₃), 3.28 (t, ³*J* = 7.5 Hz, 4H, H₅), 3.47 (t, ³*J* = 6.9 Hz, 4H, H₆), 3.66 (s, 6H, OMe), 6.71–6.77 (m, 6H, H₂ + H₁₆), 7.20 (d, ³*J* = 9.3 Hz, 2H, H₁₇), 7.35 (t, ³*J* = 7.2 Hz, 2H, H₁₂), 7.47 (t, ³*J* = 7.8 Hz, 2H, H₁₃), 7.55 (d, ³*J* = 7.8 Hz, 2H, H₁₄), 7.64 (d, ³*J* = 8.4 Hz, 4H, H₃) 8.42 (d, ³*J* = 8.1 Hz, 2H, H₁₁), 16.16 (bs, 2H, OH); (¹³C{¹H}, CDCl₃, 25 °C, vs. TMS): δ 14.55 (CH₃), 17.92 (C₅), 29.45 (Ca), 46.08 (C₆), 55.18 (OCH₃), 101.76 (C₄) 108.63 (C₈), 113.33 (C₁₆), 116.08 (C₂), 124.67 (C₁₇), 124.88 (C₁₂), 125.40 (C₁₁), 126.98 (C₁₄), 129.55 (C₁₃), 130.30 (C₁₀), 137.19 (C₁₅), 139.01 (C₃), 161.24 (C₁), 171.51 (C₉), 175.22 (C₇); (¹²⁵Te{¹H}, CDCl₃, 25 °C, vs. Me₂Te): δ 367.4. HRMS (ESI+) calc. for C₄₄H₄₆N₂O₄Te₂HgBr (M⁺–Br) 1207.0472, found *m/z* 1207.0450 (Δ 1.8098 ppm). IR(KBr, cm⁻¹): 3427, 1592, 1249, 1179, 1023, 794, 742, 691, 587, 515, 415.

2.6. Procedure for catalytic Suzuki reaction

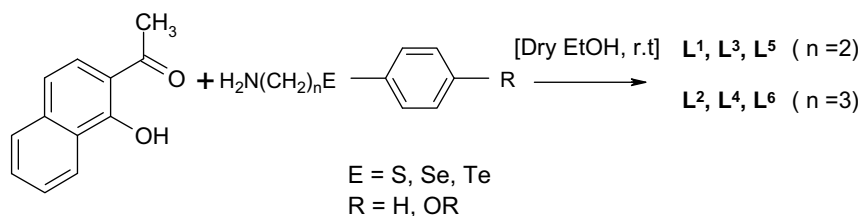
Bromobenzene or its derivative (1 mmol), benzenboronic acid (0.183 g, 1.5 mmol), K₂CO₃ (0.276 g, 2 mmol), distilled water (0.5 mL), DMF (4 mL) and catalyst (complex **1/2/3/5/6**) (0.001 mmol) were stirred together under reflux on an oil bath for 24 h at 100 °C under ambient conditions. The reaction mixture was cooled to room temperature and mixed with 20 mL of water. The product was extracted from the aqueous mixture with hexane/diethyl ether (25–50 mL). The solvent was partly evaporated on a rotary evaporator to get white crystalline solid products, which were filtered and washed with 3–4 mL of hexane. The NMR (¹H and ¹³C{¹H}) spectra and m.p.'s identified the products.

2.7. Procedure for catalytic Heck reaction

The mixture of alkene (1.5 mmol), aryl halide (1 mmol), Na₂CO₃ (0.212 g, 2.0 mmol), DMF (4.0 mL) and catalyst (complex **1/2/3/5/6**) (0.001 mmol) was stirred under reflux on an oil bath for 24 h at 100 °C under nitrogen atmosphere. It was cooled to room temperature. To obtain (*E*)-1-(4-chloro/nitrophenyl)-2-phenylethene, it was treated with chloroform (40 mL) and filtered. The filtrate was washed with water (3 × 25 mL) and evaporated on rotary evaporator. The product was further purified chromatographically (silica gel column) using hexane–ethylacetate mixture (9:1). For (*E*)-3-(4-chloro/nitrophenyl)acrylic acid the cooled reaction mixture was mixed with NaHCO₃ (0.50 g) and water (30 mL). The mixture was stirred for 1 h at room temperature. The aqueous phase was separated and acidified with 5 N HCl. On cooling to 0 °C, the solid precipitate was formed which was filtered, washed and air dried.

3. Results and discussion

The ligands L¹–L⁶ synthesized by the reactions given in Scheme 1 are stable and can be stored under ambient conditions up to 6 months easily. They have good solubility in CHCl₃, CH₂Cl₂, CH₃CN, CH₃OH, C₂H₅OH and acetone. In hexane all the ligands are sparingly soluble. They behave as non-electrolytes. The complexes **1–14** are stable under ambient conditions and soluble in CHCl₃, CH₂Cl₂, CH₃CN, EtOH, MeOH and acetone but insoluble in hexane. The stoichiometry of complexes formed by four metal ions with L¹–L⁶ does not change on varying the metal:ligand ratio. When M:L ratio is 1:2, [PdCl₂L₂] is not formed. The [PtCl(L–H)] species are not formed in case of L⁴ and L⁶ even when Pt:L ratio is 1:1. Similarly in case of L³ and L⁵, [PtCl₂L₂] is not formed when M:L is 1:2.



Scheme 1.

All of them are nonionic in nature except **11** and **12** for which the values of molar conductance at room temperature are 42.0 and 54.0 S cm² mol⁻¹, respectively, which are less than the Λ_M value (120–160 S cm² mol⁻¹) expected for a 1:1 electrolyte in MeCN, probably due to some ion association or partial change in the dentate character of ligand (from two to one). In IR spectra of all the complexes except that of **9**, **10**, **13** and **14**, $\nu_{C=N}$ stretching frequency has been observed red shifted (10–55 cm⁻¹) with respect to those of corresponding ligands indicating the involvement of its nitrogen in coordination or somewhat weaker interaction.

3.1. Ligands

In ⁷⁷Se{¹H} NMR spectra of **L³** and **L⁴** the signals appears almost at the same position (287.7 and 288.8 ppm, respectively). The signal in ¹²⁵Te{¹H} NMR spectrum of 2-(4-methoxyphenyltelluro)ethylamine gets deshielded by 72 ppm when Schiff base **L⁵** is formed but in case of **L⁶**, its position remains similar to that of precursor amine. ¹³C{¹H} NMR spectra of all the ligands were found characteristic. On comparing the spectra of six ligands, it is observed that signal of C₄ (bonded to E = S, Se or Te) is most high field in case of Te, followed by Se and S. Similar trends are observed for the signal of carbon atom of CH₂E also. The signal of –CH₃ carbon appears almost at the same position in the spectra of **L¹** to **L⁶**. The ¹H NMR spectra of all the ligands were found characteristic. The signals of H₅ protons of ligands containing E–(CH₂)₂–N system are deshielded by 0.12–0.29 ppm in comparison to those ligands containing E–(CH₂)₃–N system. The signal of –OH proton in the ¹H NMR spectra of all the ligands has been found most deshielded due to intramolecular O–H···N hydrogen bonding.

3.2. [PdCl(L–H)] complexes

The complexes **1**, **2**, **3**, **5**, **6** and **8** are of the stoichiometry [PdCl(L–H)], which is supported by crystal structures of **1**, **2**, **3** and **6** given below (Section 3.2). The chemical shifts observed in ⁷⁷Se{¹H} and ¹²⁵Te{¹H} NMR spectra of palladium(II) complexes of **L³–L⁶** and change in their positions with respect to those of corresponding ligands are compared in Table 1. The signal of **L³** in ⁷⁷Se NMR spectrum shows deshielding of 158 ppm on complexation with Pd(II), whereas in case of **L⁴** the deshielding is of the order of 8 ppm only (Table 1). This difference is due to formation of five- and six-membered rings, respectively, with **L³** and **L⁴**. On comparing P-31 NMR spectra of various metal–phosphine complexes, similar observations have been made earlier [12a]. These deshieldings on formation of complexes **3** and **5** indicate that the coordination of ligands in them occurs through Se. The deshielding of 298 ppm has been observed in the ¹²⁵Te{¹H} NMR signal of **L⁵** on the complexation with Pd(II), which is much higher than the one shown by **L⁶** on complexation with the same metal (Table 1). It may also be attributed to chelate ring size effect as mentioned in case of Se analogues. As in the case of **3** and **5** the coordination of **L⁵** and **L⁶** with Pd(II) through Te can be easily inferred from these deshieldings of signals in Te-125 NMR spectra of **6** and **8**. This is further supported by ¹³C{¹H} NMR spectral data. The signal of CH₂Te (C₅) in ¹³C{¹H}

Table 1
¹²⁵Te or ⁷⁷Se NMR signals of metal complexes of **L³–L⁶** and their shielding/deshielding

S.no.	Complex	Chemical shift δ (ppm) in ¹²⁵ Te or ⁷⁷ Se NMR	Change in chemical shift relative to ligand (ppm)
1	PdCl(L³–H) (3)	445.7	+158
2	[PtCl(L³–H)] (4)	388.6	+100.9
3	[PdCl(L⁴–H)] (5)	297	+8.2
4	[PdCl(L⁵–H)] (6)	764.1	+298
5	[PtCl(L⁵–H)] (7)	624.9	+158.8
6	[PdCl(L⁶–H)] (8)	484.8	+24.5
7	[PtCl ₂ (L⁴)₂] (9)	339.0 and 340.3	+50.2 and +51.5
8	[PtCl ₂ (L⁶)₂] (10)	550.9 and 563.1	+90.6 and +102.8
9	[(<i>p</i> -Cymene)RuCl ⁵]Cl (11)	515.3	+49.2
10	[(<i>p</i> -Cymene)RuCl ⁶]Cl (12)	535.8	+75.5
11	[HgBr ₂ (L⁵)₂] (13)	362.6	–103.5
12	[HgBr ₂ (L⁶)₂] (14)	367.4	–92.9

NMR spectrum shows deshielding of 8.42–10.82 ppm on complexation with Pd. The carbon signal of CH₂Se is deshielded between 5.56 and 6.18 ppm. The deshielding in CH₂S carbon signal on complexation (3.94–7.74 ppm) also indicates the coordination of **L¹–L²** through sulphur. The deshieldings of signal of C₄ are in the ranges 4.76–5.14, 2.1–2.9, 5.7–13.50 ppm, respectively, for E = Te, Se and S and imply the formation of Pd–chalcogen bond. In ¹³C{¹H} NMR spectra of each palladium complex the signal of –CH₃ appears deshielded (5–6 ppm) with respect to that of corresponding ligand which indicates the involvement of $\nu_{C=N}$ group in coordination with the Pd. The deshielding of signal of =NCH₂ in ¹³C{¹H} NMR spectra not only indicates coordination of Pd with $\nu_{C=N}$ group but changes with chelate ring size. When out of two chelate rings formed around the central metal atom, one ring is five-membered and the other is six-membered (**1**, **3** and **6**), the deshielding in the signal of =NCH₂ carbon is between 14.60 and 16.18 ppm, whereas when both the rings around the central metal atom are six-membered (**2**, **5** and **8**), the deshielding of signal of =NCH₂ carbon is between 8.51 and 11.47 ppm.

The signal of –OH does not appear in the ¹H NMR spectra of complexes **1**, **2**, **3**, **5**, **6** and **8** indicating the coordination of –OH group to palladium(II) in the deprotonated form (O⁻). On considering the Se-77, Te-125 and C-13 NMR data with this observation, it may be inferred that **L¹–L⁶** coordinate in uni-negative tridentate mode in all Pd-complexes as supported by single-crystal structures of **1**, **2**, **3** and **6**.

The signal of CH₃ in proton NMR spectra does not show expected deshielding uniformly for all Pd-complexes. It shows shielding (0.30–0.38 ppm) on comparing the spectra of **3** and **6** with those of corresponding ligands. In the spectra of **1**, **2** and **5**, CH₃ signal shows deshielding (0.08–0.31 ppm) with respect to those of corresponding free ligands. However, in the case of **8** the signal of CH₃ appears at a position identical to that of ligand **L⁶**. In ¹H NMR spectra the H₅ protons of all the ligands on complexation with Pd(II), show two multiplets, each corresponds to

one proton, except in case of **L**⁵ where one H₅ appears as triplet of doublet and other doublet of triplet. In all cases the signal for H₅ is expected to be 'ddd' as two protons of each CH₂ group are expected to be diastereotopic. However, due to overlap of signals such splittings are masked. Of two one signal is shielded (~0.15–0.65 ppm) and the other one deshielded (~0.17–0.51 ppm) in comparison to corresponding ligand signals, except for **8**, which exhibits both signals shielded in comparison to that of corresponding ligand, and **2** which gives only one complex multiplet at higher field relative to that of ligand. The geminal =NCH₂ protons (H₆) also give two different signals (one for each) in case of **3** and **6**. One signal is shielded (~0.07–0.23 ppm) and the other deshielded (~0.37–1.40 ppm) in comparison to those of the corresponding ligands. In the proton NMR spectra of **1**, **2**, **5** and **8**, =NCH₂ protons appear as a complex multiplet, deshielded (~0.08–0.33 ppm) with respect to those of corresponding free ligands. The proton NMR spectra are affected more by spatial interactions and conformational influences which may be responsible for some of these divergences. Therefore, **5** and **8** can also be formulated as [PdCl(L–H)] like other Pd-complexes characterized structurally.

3.3. Platinum complexes

There are two type of platinum complexes formed. It is interesting to note that on varying metal: ligand ratio same species are formed. One has composition [PtCl(L–H)] (**4** and **7**) and the other [PtCl₂(L)₂] (**9** and **10**). The later ones are supported by HRMS data. The structural diagnosis of Pt-complexes is largely based on the NMR spectral data only, as single crystals could not be grown for any Pt-complex. The deshielding of 50–100 ppm (Table 1) has been observed in ⁷⁷Se{¹H} NMR signal of **L**³ and **L**⁴ when they coordinate with Pt(II). The appearance of two very close signals in the spectrum of **9** may be due to the presence of both *cis* and *trans* isomeric forms together as it has two ligand molecules. The chemical shifts observed in the ¹²⁵Te{¹H} NMR spectra of Pt-complexes of **L**⁵ and **L**⁶ and their relative positions with respect to those of corresponding ligands are also given in Table 1. On complexation with Pt(II), the deshielding is ~158.8 ppm in case of **L**⁵ and is 90.6/102.8 for **L**⁶. The appearance of two signals takes place in the case of **L**⁶, which may be due to the presence of *cis* and *trans* forms together. Attempts made for column chromatographic separation of the isomeric forms of **9** and **10** failed. These deshieldings indicate that in **4**, **7**, **9** and **10**, **L**³–**L**⁶ coordinate with Pt(II) through Se or Te. This is supported by carbon-13 NMR data as signal of C₅ (CH₂E; E = Se or Te) in the spectra shows deshielding of 7.69, 3.69, 8.86, and 11.41/11.53 ppm in case of **4**, **7**, **9** and **10**, respectively, with respect to those of free ligands. The signal of C₄ (attached to Se or Te) also gets deshielded on the formation of **9**, **7** and **10** (1.88–4.17 ppm), supporting the coordination of ligands in the Pt-complexes through Se or Te. The signal of –CH₃ in carbon-13 NMR appears deshielded (6.43–6.77 ppm) for complexes **4** and **7** but in **9** and **10** it appears nearly at the position observed in the corresponding ligand. This probably implies that in **9** and **10** the ligands **L**⁴ and **L**⁶ do not coordinate through >C=N– group. The doubling of signals of some carbon atoms in ¹³C{¹H} NMR spectra of **9** and **10** further supports the existence of *cis*–*trans* isomeric forms inferred from Se-77 and Te-125 NMR spectra. In carbon-13 NMR of **4** and **7**, the deshielding in the signal of =NCH₂ is found between 16.67 and 16.93 ppm, respectively, whereas in case of **9** and **10**, the signal of =NCH₂ appears almost at the same position at which it appears in the corresponding ligand. This indicates that in **9** and **10**, =NCH₂ is not involved in coordination. The signal of –OH does not appear in ¹H NMR spectra of complexes **4** and **7** indicating the coordination of –OH group with Pt(II) in the deprotonated

form. However, in the proton NMR spectra of **9** and **10** signal of OH group has been observed. This rules out formulation of type [Pt(L–H)₂Cl] · 2HCl for **9** and **10**. Thus most probably in **9** and **10** the Schiff base ligands coordinate through Se or Te only (unidentate mode) and the complexes are *cis*–*trans* isomeric mixtures, whereas in **4** and **7** Schiff base ligands bind in a tridentate uninegative mode as in the case of Pd-complexes.

Proton NMR spectral data generally support the conclusions made above for **4**, **7**, **9** and **10**. In proton NMR spectrum of **9** the CH₃ protons give four singlets of similar heights. This is due to its existence as a *cis*–*trans* isomeric mixture and probably also contributed by non-equivalence of the two Schiff base ligand molecules in each isomer. In mass spectra of **9** and **10** appearance of [M⁺–2Cl] peak suggest that there are other interactions in these molecules which make Pt–Cl bond weak and probably make two ligands non-equivalent. The possibility of impurity in the samples of **9** and **10** was ruled out on the basis of elemental analysis and mass spectra. In ¹H NMR spectra, both the geminal H₅ protons of **4** as well as **7** appear at different positions. In case of **7**, one H₅ proton signal appears shielded (0.87 ppm) and the other one deshielded (~0.44 ppm) in comparison to that of ligand but in case of **4**, both the signals are deshielded (0.06 and 0.67 ppm). On complexation of **L**⁴ and **L**⁶ with Pt(II) signals for H₅ protons appear overlapped with those of H₆ protons. The proton NMR spectrum of **10** exhibits double number of signals for some protons. This further supports the existence of this complex as a *cis*–*trans* isomeric mixture. In ¹H NMR spectra of **7** the two geminal =NCH₂ protons (H₆) give two different signals (one for each). One signal is shielded (0.35 ppm) and the other deshielded (0.84 ppm) in comparison to that of the corresponding ligand. But in case of **4**, **9** and **10**, =NCH₂ protons appear as a complex multiplet, overlapped with other signals so shielding or deshielding cannot be quantified explicitly. The **L**⁴ and **L**⁶ ligate with Pd and Pt differently due to several reasons. The Pt–Cl bond is more covalent and strong than Pd–Cl bond which makes its reactivity lower towards OH group. The Pt(II) is more 'Soft' Lewis acid than Pd(II) therefore its coordination with N of >C=N resulting in six-membered ring does not become very stable. Consequently **L**⁴ and **L**⁶ ligate through Se or Te only.

3.4. Ruthenium complexes

The single crystals could not be grown for any Ru-complex. Therefore for species [Ru(*p*-cymene)Cl(L⁵/L⁶)]Cl, NMR spectral data (with support of mass) are mainly correlated with the possible structural features. On complexation with ruthenium **L**⁵ and **L**⁶ show deshielding in Te-125 NMR spectra (Table 1). It is 49.2 ppm in the case of **L**⁵ and 75.5 ppm when **L**⁶ coordinates with Ru(II). In ¹³C{¹H} NMR spectra of **11** and **12** the signals of CH₂Te (C₅) show deshielding (11.07 and 9.94 ppm, respectively) in comparison to those of free ligands. The signal of C₄ carbon atom also appears deshielded (6–7 ppm) in both **11** and **12** with respect to those of corresponding ligands. Thus ligation of **L**⁵ and **L**⁶ with Ru through Te may be inferred. In ¹³C{¹H} NMR spectra, the position of signal of –CH₃ carbon remains almost unchanged on the formation of **11** and **12**. Moreover in ¹³C{¹H} NMR spectra of **11** and **12**, =NCH₂ carbon signal shows shielding (up to ~3 ppm). This suggest that >C=N group does not coordinate strongly with Ru. A strong association between complex and chloride ion, facilitated by weak interaction between Ru and >C=N group, seems to lower conductance values for **11** and **12**. The appearance of [M⁺–Cl] peak in HRMS concurs with this proposition. In ¹H NMR spectra of **11** as well as **12**, the presence of signal of OH proton indicates that –OH group does not coordinate with metal. In ¹H NMR spectra of **11** and **12** both the geminal H₅ protons show two multiplets (one for each) but both are deshielded

Table 2
Crystal data and structural refinements for **L**¹, **L**³ and **L**⁶

Compound	L ¹	L ³	L ⁶
Empirical formula	C ₂₀ H ₁₉ NOS	C ₂₀ H ₁₉ NOSe	C ₂₂ H ₂₃ NO ₂ Te
Formula weight	321.43	368.32	461.0
Crystal size (mm)	0.407 × 0.289 × 0.196	0.463 × 0.215 × 0.167	0.423 × 0.298 × 0.178
Crystal system	Triclinic	Triclinic	Triclinic
Space group	P1	P1	P1
Unit cell dimensions			
<i>a</i> (Å)	7.8504(15)	8.0693(14)	6.3152(5)
<i>b</i> (Å)	10.336(2)	10.2505(17)	8.7203(7)
<i>c</i> (Å)	11.594(2)	11.5208(19)	18.3132(14)
β (°)	73.700(3)	72.878(4)	85.8362(11)
Volume (Å ³)	834.7(3)	842.6(2)	976.85(13)
Z	2	2	2
<i>D</i> _{calc.} (Mg m ⁻³)	1.279	1.440	1.567
Absorption coefficient (mm ⁻¹)	0.198	2.232	1.538
<i>F</i> (000)	340.00	376.00	460.0
θ Range (°)	1.84–25.49	1.85–28.32	2.23–25.49
Index ranges	–9 ≤ <i>h</i> ≤ 9 –12 ≤ <i>k</i> ≤ 12 –14 ≤ <i>l</i> ≤ 14	–10 ≤ <i>h</i> ≤ 10 –13 ≤ <i>k</i> ≤ 13 –15 ≤ <i>l</i> ≤ 15	–7 ≤ <i>h</i> ≤ 7 –10 ≤ <i>k</i> ≤ 10 –22 ≤ <i>l</i> ≤ 22
Reflections collected	8365	10087	9616
Independent reflections (<i>R</i> _{int})	3096(0.0983)	4014(0.0965)	3610(0.0205)
Completeness to maximum θ (%)	99.7	95.8	98.8
Maximum/minimum transmission	0.965/0.931	0.645/0.456	0.764/0.581
Data/restraints/parameters	3096/0/209	4014/0/210	3610/0/254
Goodness-of-fit on <i>F</i> ²	1.061	0.907	1.064
Final <i>R</i> indices [<i>I</i> > 2 σ (<i>I</i>)]	<i>R</i> ₁ = 0.0564, <i>wR</i> ₂ = 0.1469	<i>R</i> ₁ = 0.0577, <i>wR</i> ₂ = 0.0990	<i>R</i> ₁ = 0.0251, <i>wR</i> ₂ = 0.0660
<i>R</i> indices (all data)	<i>R</i> ₁ = 0.0603, <i>wR</i> ₂ = 0.1529	<i>R</i> ₁ = 0.0964, <i>wR</i> ₂ = 0.1110	<i>R</i> ₁ = 0.0270, <i>wR</i> ₂ = 0.0671
Largest difference in peak/hole (e Å ⁻³)	0.462/–0.333	0.621/–0.526	0.436/–0.385

Table 3
Crystal data and structural refinements for **1**, **2**, **3** and **6**

Compound	1	2	3	6
Empirical formula	C ₂₀ H ₁₈ ClNOPdS	C ₂₁ H ₂₀ ClNOPdS	C ₂₀ H ₁₈ ClNOPdSe	C ₂₁ H ₂₀ ClNO ₂ PdTe
Formula weight	462.26	476.32	509.18	664.74
Crystal size (mm)	0.52 × 0.18 × 0.15	0.298 × 0.165 × 0.076	0.463 × 0.215 × 0.167	0.34 × 0.28 × 0.26
Crystal system	Triclinic	Monoclinic	Monoclinic	Orthorhombic
Space group	P1	P2(1)/c	P2(1)/c	C2cb
Unit cell dimensions				
<i>a</i> (Å)	9.689(2)	16.038(9)	9.6820(14)	9.7664(3)
<i>b</i> (Å)	12.429(4)	10.536(6)	12.2362(18)	16.1747(6)
<i>c</i> (Å)	15.677(4)	12.351(7)	15.813(2)	27.8791(9)
β (°)	77.09(2)	110.369(11)	101.645(2)	90.00(2)
Volume (Å ³)	1838.4(9)	1956.5(19)	1834.8(4)	4404.0(3)
Z	4	4	4	8
<i>D</i> _{calc.} (Mg m ⁻³)	1.670	1.617	1.843	2.005
Absorption coefficient (mm ⁻¹)	1.276	1.201	3.148	2.525
<i>F</i> (000)	928.0	960.0	1000.0	2568.0
θ Range (°)	4.49–32.57	1.35–28.32	2.12–25.50	3.28–25.00
Index ranges	–14 ≤ <i>h</i> ≤ 14 –18 ≤ <i>k</i> ≤ 18 –23 ≤ <i>l</i> ≤ 22	–21 ≤ <i>h</i> ≤ 21 –14 ≤ <i>k</i> ≤ 14 –16 ≤ <i>l</i> ≤ 16	–11 ≤ <i>h</i> ≤ 11 –14 ≤ <i>k</i> ≤ 14 –19 ≤ <i>l</i> ≤ 19	–11 ≤ <i>h</i> ≤ 11 –17 ≤ <i>k</i> ≤ 19 –32 ≤ <i>l</i> ≤ 33
Reflections collected	28871	11519	17812	12537
Independent reflections (<i>R</i> _{int})	12020 (0.0371)	4850 (0.1000)	3412 (0.0377)	3851 (0.0274)
Completeness to maximum θ (%)	89.9	99.5	100.0	1.86(0.99)
Maximum/minimum transmission	0.82300/0.75740	0.915/0.787	0.593/0.445	0.521/0.429
Data/restraints/parameters	12020/0/453	4850/0/200	3412/0/227	3851/1/270
Goodness-of-fit on <i>F</i> ²	1.111	1.318	1.230	1.068
Final <i>R</i> indices [<i>I</i> > 2 σ (<i>I</i>)]	<i>R</i> ₁ = 0.0636, <i>wR</i> ₂ = 0.1782	<i>R</i> ₁ = 0.0796, <i>wR</i> ₂ = 0.1705	<i>R</i> ₁ = 0.0295, <i>wR</i> ₂ = 0.0744	<i>R</i> ₁ = 0.0406, <i>wR</i> ₂ = 0.0953
<i>R</i> indices (all data)	<i>R</i> ₁ = 0.0883, <i>wR</i> ₂ = 0.1903	<i>R</i> ₁ = 0.0929, <i>wR</i> ₂ = 0.1869	<i>R</i> ₁ = 0.0343, <i>wR</i> ₂ = 0.0781	<i>R</i> ₁ = 0.0475, <i>wR</i> ₂ = 0.0985
Largest difference peak/hole (e Å ⁻³)	2.551/–1.114	0.676/–1.248	0.454/–0.360	1.764/–1.916

(~0.22–0.59 ppm) in comparison to those of corresponding free ligands. This supports the binding of ligands **L**⁵ and **L**⁶ with Ru(II) through Te. In ¹H NMR spectra of **11**, the geminal =NCH₂ protons signal overlaps with the signal of OMe and consequently its shielding/deshielding cannot be quantified. But in the case of **12**, =NCH₂ protons appear as a complex multiplet, little deshielded (~0.023 ppm) with respect to those of corresponding free ligands. This supports the possibility of weak interaction between Ru and >C=N group as suggested above but also suggest that

Schiff base ligands in **11** and **12** both are behaving as a monodentate ligand.

3.5. Mercury complexes

Single crystals could not be grown for any Hg-complex also. Contrary to deshielding (Table 1) observed in ¹²⁵Te(¹H) NMR signal of **L**⁵ and **L**⁶ on complexation with Pd(II), Pt(II) and (*p*-cymene)-Ru(II), there is a shielding of 103.5 ppm when **L**⁵ complexes with

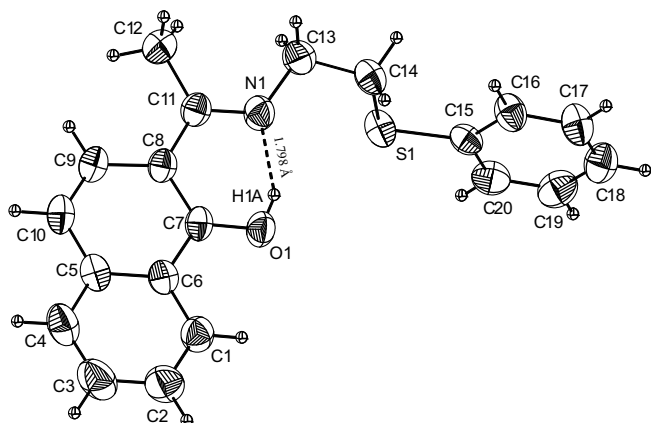


Fig. 1. ORTEP diagram of **L**¹ with 50% probability ellipsoids.

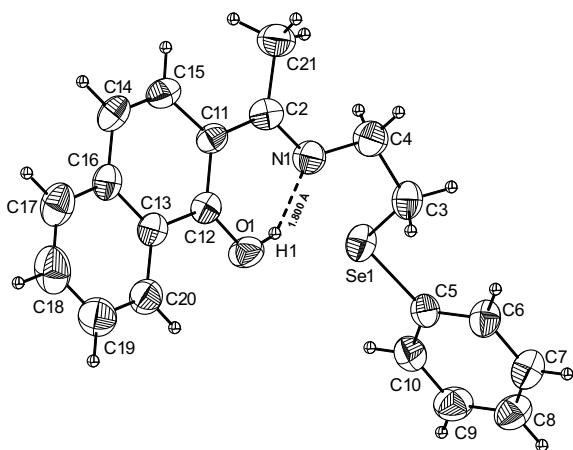


Fig. 2. ORTEP diagram of **L**³ with 50% probability ellipsoids.

Hg(II) (Table 1). The shielding is however less (~93 ppm) in case of **L**⁶. For a d¹⁰ system such shieldings have been reported earlier as well [12b–d].

In ¹³C{¹H} NMR spectra of both **13** and **14**, the signal of –CH₃ carbon appears almost at the same position at which it appears in **L**⁵ and **L**⁶, respectively. However, signal of CH₂Te (C₅) shows deshielding of 14.37 and 13.14 ppm in the carbon-13 NMR spectra of **13** and **14**, respectively, in comparison to those of free ligands. The signal of C₄ also gets deshielded by 2.51 ppm in the spectra of **13** and 2.03 ppm in the case of **14**. These deshieldings in the position of signals of C₄ and C₅ on complex formation imply the for-

mation of metal–chalcogen bond. In ¹³C{¹H} NMR spectra the position of signal of =NCH₂ has been found deshielded (2.06 ppm) when **13** is formed while it appears exactly at the same position in **14** at which it appears in the spectrum of free ligand **L**⁶. Thus possibility of existence of weak interaction between Hg and >C=N group cannot be ruled out completely. In the ¹H NMR spectra of both **13** and **14**, –OH appears indicating that –OH group does not coordinate with metal. High resolution mass spectra supports metal to ligand ratio as 1:2, which suggest that ligands are bonded with Hg, mainly through Te and weak interactions with N of >C=N group may exist.

In the ¹H NMR spectra of both **13** and **14**, a triplet just like that of ligand appears for H₅ protons. This triplet is deshielded by 0.50 ppm in case of **13** and 0.40 ppm in case of **14** in comparison to that of corresponding ligand. In ¹H NMR spectra the position of =NCH₂ proton signal has been found deshielded (0.21 ppm) in case of **13** while it appears almost at the same position in **14** at which it appears in the spectrum of free **L**⁶. This supports the possibility of weak interactions between Hg and >C=N group, particularly in the case of **13**.

3.6. Crystal structures

The crystal structures of **L**¹, **L**³, **L**⁶, **1**, **2**, **3** and **6** were solved. Crystal data and structural refinements are given in Tables 2 and 3. Molecular structures of **L**¹, **L**² and **L**³ are shown in Figs. 1–3, respectively, and their bond lengths and angles are available as Supplementary material. The S–C, Se–C and Te–C bond lengths 1.7648(19)/1.801(2), 1.915(3)/1.942(3) and 2.116(2)/2.160(3) Å, respectively, are consistent with the earlier reports [13–15]. The order of E–C(alkyl/aryl) bond distances is S < Se < Te. The E–C(aryl) bond distances (E = S, Se and Te) are somewhat shorter than E–C(alkyl) distances in all the three ligands **L**¹, **L**² and **L**³. The C(alkyl)–S–C(aryl) bond angle was found to be maximum 102.67(9)° followed by C(alkyl)–Se–C(aryl) 99.23(15)° and C(alkyl)–Te–C(aryl) 95.15(9)°. The intramolecular hydrogen bonding O–H...N have been observed in the structure of all the three ligands **L**¹, **L**³ and **L**⁶.

The molecular structures of **1** and **2** are shown in Fig. 4 and Fig. 5, respectively, and their selected bond distances and angles are given in Table 4. The unit cell has nearly similar two molecules of **1**. Their slightly different bond lengths and bond angles are indexed as A and B in the Table 4. The geometry around Pd is square planar in **1** as well as **2**. The ligands are coordinated with Pd in a monoanionic tridentate (S, N, O[−]) mode in both the complexes. This kind of coordination mode forms a six-membered chelate ring with O[−] and N (azomethine) and a five-membered ring with S and N (azomethine) in case of **1** but both the rings are six-membered in case of **2**. The Pd–S bond length in **1** (2.2704(16) Å/2.2631(16) Å)

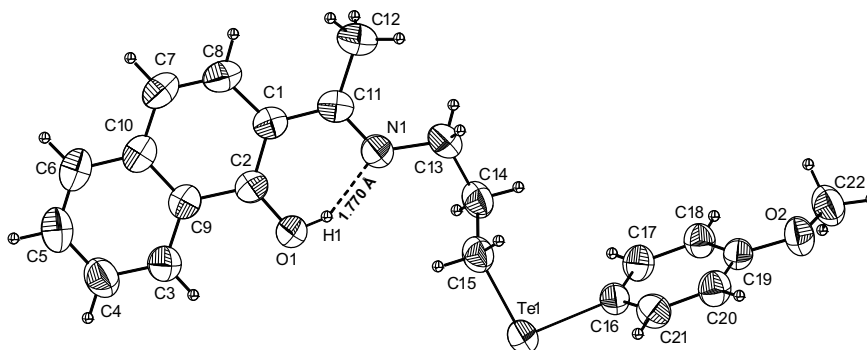
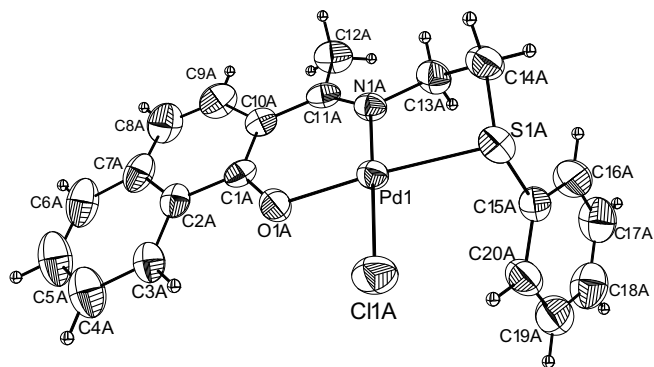
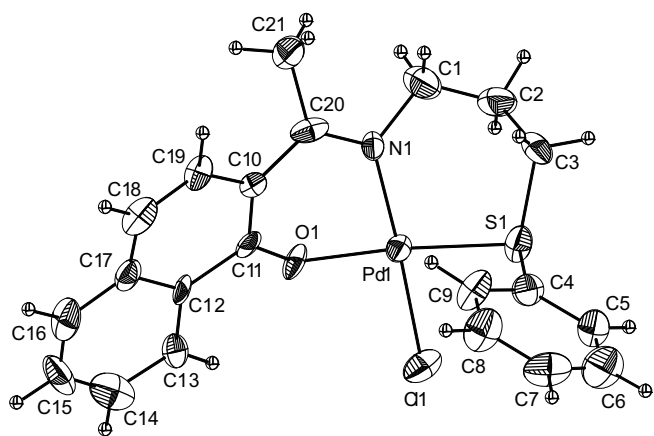


Fig. 3. ORTEP diagram of **L**⁶ with 50% probability ellipsoids.

Fig. 4. ORTEP diagram of **1** with 50% probability ellipsoids.Fig. 5. ORTEP diagram of **2** with 50% probability ellipsoids.

and **2** (2.266(4) Å) are similar. The Pd–N bond lengths of 2.019(5)/2.012(5) and 2.015(10) Å, respectively, in **1** and **2** are little higher than that of 1.965(2) Å reported [16] for [PdCl{EtNHC(=S)NH–N=CH–C₆H₄–2–O[–]}], but the Pd–O distances of 1.982(4)/1.987(4) and 1.998(8) Å in **1** and **2**, respectively, are comparable to 2.019(2) Å reported [16] for [PdCl{EtNHC(=S)NH–N=CH–C₆H₄–2–O[–])]. The Pd–S bond distances, 2.2704(16)–2.2631(16) Å and Pd–Cl bond distances, 2.3290(15)–2.309(4) Å of **1** and **2** are consistent with the values [16] reported for [PdCl{EtNHC(=S)NH–N=CH–C₆H₄–2–O[–]}] [Pd–S = 2.2456(9) Å and Pd–Cl = 2.3078(8) Å] and [PdCl₂{4–MeOC₆H₄TeCH₂CH₂SEt}] [Pd–S = 2.268(4) Å and Pd–Cl = 2.316(4) Å] [17]. The Pd–S bond distance observed in *cis*-Pd(SNNMe₂–S)(AsPh₃)Cl₂ (2.249(1) Å) [18] is also in agreement with Pd–S bond distances of **1** and **2**. In *trans*-[Pd(SCN)₂]P(OPh)₃]₂ the Pd–S bond length is reported [19] as 2.352 Å, longer than that of **1** and **2**, probably due to the *trans* influence of S. The metal–ligand bond lengths of **1** and **2** are also consistent with the sum of the covalent radii for Pd–Cl, Pd–N, Pd–O and Pd–S (2.27, 2.03, 2.01 and 2.30 Å, respectively).

The molecular structure of **3** is shown in Fig. 6. The selected bond lengths and angles are given in Table 4. The ligand is coordinated with Pd in a monoanionic tridentate (Se, N, O[–]) mode forming a six-membered chelate ring with O[–] and N (azomethine) and a five-membered ring with Se and N (azomethine) around the central metal atom. The Pd–Se, Pd–N, Pd–O and Pd–Cl bond distances, 2.3600(5) Å, 2.010(3), 1.973(2) and 2.3156(9) Å, respectively, of **3** are consistent with the earlier reports [14] for [PdCl{PhSe–(CH₂)₂–N=C(CH₃)–C₆H₄–2–O[–]}] [Pd–Se = 2.3669(11) Å, Pd–N = 2.003(7), Pd–O = 1.977(6) and Pd–Cl = 2.305(2) Å] and [PdCl{PhSe–(CH₂)₂–N=C(CH₃)–C₆H₃–3–R–2–O[–]}] [R = CH(CH₂CH₃)₂; Pd–Se = 2.365(1) Å, Pd–N = 1.985(4), Pd–

Table 4
Bond length (Å) and bond angle (°) of (**1**), (**2**), (**3**) and (**7**)

	Bond length		Bond angle	
1	Pd(1)–O(1A)	1.982(4)	O(1A)–Pd(1)–N(1A)	91.99(18)
	Pd(2)–O(1B)	1.987(4)	O(1B)–Pd(2)–N(1B)	91.92(18)
	Pd(1)–N(1A)	2.019(5)	O(1A)–Pd(1)–S(1A)	176.17(14)
	Pd(2)–N(1B)	2.012(5)	O(1B)–Pd(2)–S(1B)	177.25(13)
	Pd(1)–S(1A)	2.2704(16)	N(1A)–Pd(1)–S(1A)	89.82(15)
	Pd(2)–S(1B)	2.2631(16)	N(1B)–Pd(2)–S(1B)	89.29(14)
	Pd(1)–Cl(1A)	2.3290(15)	O(1A)–Pd(1)–Cl(1A)	88.06(13)
	Pd(2)–Cl(1B)	2.3219(15)	O(1B)–Pd(2)–Cl(1B)	88.85(13)
	S(1A)–C(15A)	1.807(6)	N(1A)–Pd(1)–Cl(1A)	178.51(14)
	S(1B)–C(15B)	1.784(6)	N(1B)–Pd(2)–Cl(1B)	178.65(13)
	S(1A)–C(14A)	1.817(7)	S(1A)–Pd(1)–Cl(1A)	90.23(6)
	S(1B)–C(14B)	1.826(6)	S(1B)–Pd(2)–Cl(1B)	89.99(6)
	O(1A)–C(1A)	1.298(6)	C(15A)–S(1A)–C(14A)	103.9(3)
	O(1B)–C(1B)	1.303(7)	C(15B)–S(1B)–C(14B)	102.7(3)
	N(1A)–C(11A)	1.295(8)	C(15A)–S(1A)–Pd(1)	103.81(19)
	N(1B)–C(11B)	1.301(7)	C(15B)–S(1B)–Pd(2)	106.9(2)
	N(1A)–C(13A)	1.486(7)	C(14A)–S(1A)–Pd(1)	94.8(2)
	N(1B)–C(13B)	1.484(7)	C(14B)–S(1B)–Pd(2)	96.0(2)
			C(1A)–O(1A)–Pd(1)	126.0(4)
			C(1B)–O(1B)–Pd(2)	124.5(3)
			C(11A)–N(1A)–C(13A)	120.0(5)
			C(11B)–N(1B)–C(13B)	120.6(5)
			C(11A)–N(1A)–Pd(1)	126.6(4)
		C(11B)–N(1B)–Pd(2)	125.7(4)	
		C(13A)–N(1A)–Pd(1)	113.4(4)	
		C(13B)–N(1B)–Pd(2)	113.7(4)	
2	Pd(1)–O(1)	1.998(8)	O(1)–Pd(1)–N(1)	87.5(4)
	Pd(1)–N(1)	2.015(10)	O(1)–Pd(1)–S(1)	174.9(3)
	Pd(1)–S(1)	2.266(4)	N(1)–Pd(1)–S(1)	97.5(3)
	Pd(1)–Cl(1)	2.309(4)	O(1)–Pd(1)–Cl(1)	89.3(2)
	N(1)–C(20)	1.305(16)	N(1)–Pd(1)–Cl(1)	176.6(3)
	N(1)–C(1)	1.495(16)	S(1)–Pd(1)–Cl(1)	85.67(14)
	O(1)–C(11)	1.287(15)	C(20)–N(1)–C(1)	116.0(11)
	S(1)–C(4)	1.792(14)	C(20)–N(1)–Pd(1)	121.5(8)
	S(1)–C(3)	1.830(14)	C(1)–N(1)–Pd(1)	122.3(9)
			C(11)–O(1)–Pd(1)	115.2(8)
			C(4)–S(1)–C(3)	103.9(7)
			C(4)–S(1)–Pd(1)	106.4(5)
			C(3)–S(1)–Pd(1)	105.5(5)
3	Pd(1)–Cl(1)	2.3156(9)	O(1)–Pd(1)–N(1)	92.57(11)
	Pd(1)–N(1)	2.010(3)	O(1)–Pd(1)–Cl(1)	88.63(7)
	Pd(1)–O(1)	1.973(2)	N(1)–Pd(1)–Cl(1)	178.78(9)
	Pd(1)–Se(1)	2.3600(5)	O(1)–Pd(1)–Se(1)	175.43(7)
	Se(1)–C(14)	1.952(4)	N(1)–Pd(1)–Se(1)	90.49(9)
	Se(1)–C(15)	1.935(4)	Cl(1)–Pd(1)–Se(1)	88.32(3)
	N(1)–C(11)	1.308(4)	C(15)–Se(1)–C(14)	100.19(16)
	N(1)–C(13)	1.488(5)	C(15)–Se(1)–Pd(1)	99.43(11)
			C(14)–Se(1)–Pd(1)	91.64(12)
			C(11)–N(1)–Pd(1)	125.5(2)
			C(13)–N(1)–Pd(1)	114.8(2)
			C(1)–O(1)–Pd(1)	125.6(2)
	6	Pd(1)–N(1)	1.996(7)	N(1)–Pd(1)–O(1)
Pd(1)–O(1)		2.061(6)	N(1)–Pd(1)–Cl(1)	177.0(2)
Pd(1)–Cl(1)		2.293(2)	O(1)–Pd(1)–Cl(1)	92.59(16)
Pd(1)–Te(1)		2.5025(7)	N(1)–Pd(1)–Te(1)	89.2(2)
O(1)–C(1)		1.311(11)	O(1)–Pd(1)–Te(1)	176.65(15)
O(2)–C(18)		1.343(10)	Cl(1)–Pd(1)–Te(1)	88.30(6)
O(2)–C(19)		1.430(11)	C(15)–Te(1)–C(14)	96.2(3)
N(1)–C(11)		1.298(11)	C(15)–Te(1)–Pd(1)	102.3(2)
N(1)–C(13)		1.488(10)	C(14)–Te(1)–Pd(1)	89.0(2)
Te(1)–C(14)		2.150(8)	C(11)–N(1)–C(13)	121.7(7)
Te(1)–C(15)		2.133(9)	C(11)–N(1)–Pd(1)	123.9(6)
			C(13)–N(1)–Pd(1)	114.2(5)
			C(1)–O(1)–Pd(1)	114.9(5)
			C(18)–O(2)–C(19)	118.6(7)

O = 2.017(4) and Pd–Cl = 2.323(2) Å [14b]. The Pd–N, Pd–O and Pd–Cl bond distances of **3** are also consistent with the earlier reports [Pd–N = 2.01(1) Å, Pd–O = 2.03(1) Å, Pd–Cl = 2.290(4) Å] on Pd(II) complex of a tridentate ligand of (Te, N, O[–]) type [20]. The Pd–Se bond length of complex **3**, 2.3600(5) Å is shorter than those reported for

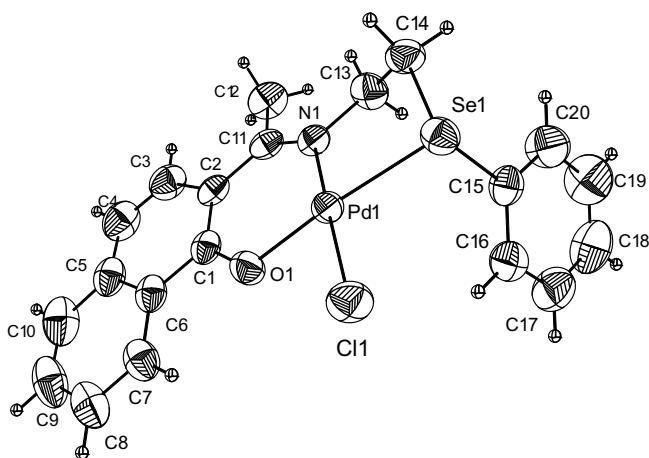


Fig. 6. ORTEP diagram of **3** with 50% probability ellipsoids.

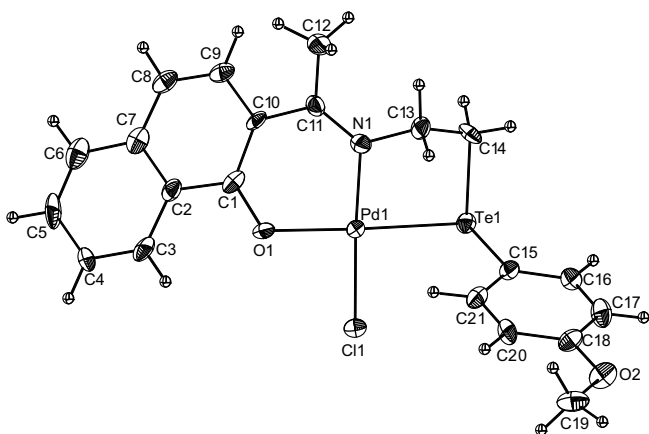
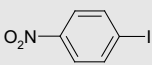
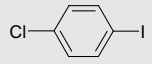
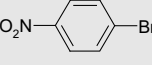
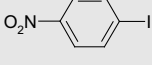
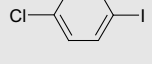
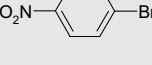


Fig. 7. ORTEP diagram of **6** with 50% probability ellipsoids.

[Pd(PEt₃)₂(SePh)(PO(OPh)₂)] (2.518(9) Å) [21] and [Pd(Me₂PCH₂CH₂-PMe₂)(Me)(SeC₆H₄-4-Cl)] (2.4483(8) Å) [22]. The possible reason for shortening of Pd–Se bond in **3** may be the tridentate nature of ligand **L**³ which makes two chelate rings and forces Se to bind with Pd(II) somewhat strongly in comparison to those complexes in which selenium ligand is monodentate one. Similar observation has been made for (N, Se, O[−]) ligands earlier [14]. The bond angles at N are consistent with their trigonal pyramidal geometry.

The ORTEP diagram of **6** given in Fig. 7 reveals its molecular structure. The selected bond lengths and angles are given in Table 5. In this case also the ligand is coordinated with Pd in a monoanionic tridentate (Te, N, O[−]) mode forming a six-membered chelate ring with O[−] and N (azomethine) and a five-membered ring with Te and N (azomethine) around the central metal atom. The lengths of Pd–Te, Pd–N, Pd–O and Pd–Cl bonds of **6**, 2.5025(7), 1.996(7), 2.061(6), 2.293(2) Å, respectively, are consistent with the earlier reports [20] for [PdCl{MeO–C₆H₄–Te–(CH₂)₂–N=C(CH₃)–C₆H₄–2–O[−]}] [Pd–Te = 2.504(1), Pd–N = 2.01(1), Pd–O = 2.03(1) and Pd–Cl = 2.290(4) Å]. The Pd–Te bond length in the present complex 2.5025(7) Å is shorter in comparison to earlier reports, 2.5873(2) [23] in di[bis(2-[1,3-dioxan-2-yl]ethyl)telluride]dichloro palladium(II) and 2.5865(2)–2.6052(2) [24] in di[N-(2-(4-methoxyphenyl)telluro)ethyl]morpholine]dichloropalladium(II) [PdCl₂(OC₄H₈-N-(CH₂)₂-Te-C₆H₄-*p*-OMe)₂]. This appears due to combined effect of tridentate nature of hybrid organotellurium ligand and the absence of strong *trans* influence in the present complex molecule. On comparing Pd–N, Pd–O, Pd–Cl, Pd–Se and Pd–Te bond lengths

Table 5
Conversions (%) in Suzuki and Heck reactions

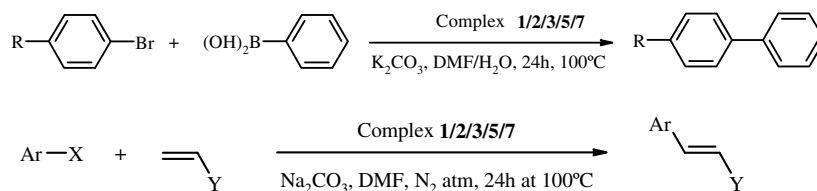
Substituents on reactants		Conversion (%)				
		1	2	3	5	6
R		Suzuki reaction				
OMe		25	10	15	10	10
H		45	20	40	25	40
NO ₂		80	70	85	82	75
Ar–X		Y				
		Heck reaction				
	COOH	78	68	80	72	75
	COOH	70	65	74	68	65
	COOH	35	25	38	30	32
	Ph	75	68	78	70	75
	Ph	78	60	70	65	75
	Ph	30	32	35	30	32

with sum of their covalent radii 2.03, 2.01, 2.27, 2.44 and 2.64 Å, respectively, the bonding between **L**³/**L**⁵ and Pd seems to be strong in nature. The geometry around chalcogen atoms in **1**, **2**, **3** and **6** is pyramidal.

It is interesting to note the effect on bond lengths/angles of chalcogenated Schiff bases when they coordinate with metal ions. The C(alkyl)–S–C(aryl) bond angle in **L**¹ is 102.67(9)^o and remains almost unchanged on the formation of **1** (102.7(3)^o/103.9(3)^o). Similarly is the case with **L**³ C(alkyl)–Se–C(aryl) bond angle is 99.23(15)^o and becomes 100.19(16)^o on the formation of **3**. The S–C(aryl) and S–C(alkyl) bond distances in **L**¹ are 1.7648(19) and 1.801(2) Å, respectively, but on formation of **1**, the distances for these bonds get increased to 1.807(6)/1.784(6) and 1.817(7)/1.826(6) Å, respectively. Similarly, the Se–C(aryl) and Se–C(alkyl) bond distances in **L**³ are 1.915(3) and 1.942(4) Å, respectively, but on formation of **3**, the distances for these bonds becomes 1.935(4) and 1.952(4) Å, respectively. The >C=N– bond distances in **L**¹ and **L**³ are 1.304(2) and 1.314(4) Å, respectively. However, these distances remains almost unchanged on complexation with Pd(II) [1.295(8)/1.301(7) and 1.308(4) Å, respectively, in **1** and **3**]. However, N–CH₂ bond distance [1.467(2) and 1.472(4) Å, respectively, in **L**¹ and **L**³] gets slightly increased on the formation of **1** and **3** and becomes 1.486(7)/1.484(7) and 1.488(5) Å, respectively. The O–C distances, 1.276(2) and 1.285(4) Å, respectively, for **L**¹ and **L**³ also get slightly increased on the formation of **1** and **3** and become 1.298(6)/1.303(7) and 1.303(4) Å, respectively.

3.7. Applications in Suzuki and Heck reactions

The Suzuki and Heck reaction were carried out using complexes **1**–**3**, **5** and **6** as summarized in Scheme 2. The percentage conversions were found up to 85 (Table 5). Heck reaction is among the most



Scheme 2.

powerful tools in organic synthesis for carbon–carbon bond formation. The complexes used as catalysts are based on phosphorus ligands as well as involve phosphorus-free ligands. The improved catalytic activity of transition metal complexes with hemilabile ligands has been reported [25]. But many phosphine based catalysts are often water- and air-sensitive. Therefore, catalysis under phosphine-free conditions is a challenge of high importance, and a number of Pd-complexes of phosphine-free ligands [26] have been reported to exhibit promising catalytic activity for Heck reaction. Recently Pd–Se bond containing complexes [27] have been found very promising for Heck reaction. This has motivated us to examine palladium(II) complexes **1–3**, **5** and **6** of tridentate chalcogenated Schiff bases [(N, O, E) type ligands, where E = S, Se or Te]. The advantage of using complexes of **1–3**, **5** and **6** is that they are air stable and also not moisture sensitive. Investigations on Pd(II) complexes of a tellurated ligand for Heck reaction have been made for the first time. A good selectivity for *trans*-products has been observed. The catalytic activity depends on the halide, while electron-withdrawing groups on the aryl ring increase the reaction rate. The reactivity decreases drastically in the order ArI > ArBr > ArCl. For Aryl bromides (1 mmol) also, a very little amount (0.001 mmol) of complex was sufficient to catalyze the Heck reaction.

Suzuki–Miyaura reaction, is also among the most important palladium-catalyzed cross-coupling reactions of both academic and industrial interest. [28–29]. In view of air and moisture sensitivity of complexes of phosphorus ligands there is an interest in phosphine-free ligands for the Suzuki–Miyaura reaction. Complexes **1–3**, **5** and **6** offer the advantage of stability under ambient conditions for Suzuki–Miyaura reactions of aryl bromides with phenylboronic acid which were carried out under aerobic conditions at 100 °C for 24 h, using K₂CO₃ as base, without addition of free ligand or any promoting additive and in the presence of a small amount of water (~one equivalent with respect to the substrates). Homocoupling of phenylboronic acid to give unsubstituted biphenyl was negligible. The reaction was performed using a 1:1000 catalyst: aryl halide molar ratio. The catalytic activity depended on the halide, while electron-withdrawing groups on the aryl ring increased the reaction rate. The activity follows in the order NO₂ > H > OMe. The conversions were found up to 85%, particularly for activated 1-bromo-4-nitrobenzene the conversions were usually about 80% or higher. The use of aryl chlorides as substrates remains the goal in cross-coupling reactions due to their inexpensive cost and convenient availability, but unfortunately, the oxidative addition in these cases is difficult due to the comparatively high C–Cl bond strength. Evaluation of palladium complexes of tellurated Schiff base ligand in the Suzuki–Miyaura reaction has also been made for the first time and results are promising. Thus chalcogenated Schiff bases of 1'-hydroxy-2'-acetonaphthone (HAN) may result in efficient catalysts for Suzuki–Miyaura cross-coupling and Heck reactions.

4. Conclusion

Schiff bases of 1'-hydroxy-2'-acetonaphthone having S, Se and Te functionalities are synthesized and compared for the first time. Their complexation with Pt(II) becomes different when value of

'n' in the ligand backbone >C=N–(CH₂)_n–E changes from 2 to 3. In Se-77 and Te-125 NMR spectra of Pd(II)/Pt(II) complexes shift of signal relative to free ligand depends on the size of chelate ring (five-membered > six-membered). The Pd–N, Pd–O, Pd–Cl, Pd–S, Pd–Se and Pd–Te bond lengths observed in the crystal structures of Pd-complexes of these Schiff bases are very close to the sum of their covalent radii, indicating strong binding of uni-negative tridentate ligands with Pd(II). The complexes of **1–3**, **5** and **6** have been found promising for homogeneous catalysis of Heck and Suzuki reactions. The advantage of using them is that they are air stable and also not moisture sensitive. A 1:1000 catalyst: aryl halide molar ratio was found optimum for Heck as well as Suzuki reactions.

Acknowledgements

Authors thank Department of Science and Technology (India) for research Project No. SR/S1/IC–23/06 and for partial financial assistance given to establish single-crystal X-ray diffraction facility at IIT Delhi, New Delhi (India) under its FIST programme. A.K. thanks Council of Scientific and Industrial Research (India) for the award of Junior/Senior Research Fellowship.

Appendix A. Supplementary material

CCDC 685767, 685768, 685769, 685770, 685771, 661338 and 685772 contain supplementary crystallographic data for **L¹**, **L³**, **L⁶**, **1**, **2**, **3** and **7**. These data can be obtained free of charge from The Cambridge Crystallographic Data Centre via www.ccdc.cam.ac.uk/data_request/cif. Supplementary data associated with this article can be found, in the online version, at [doi:10.1016/j.jorganchem.2008.07.024](https://doi.org/10.1016/j.jorganchem.2008.07.024).

References

- [1] A. Douhal, Acc. Chem. Res. 37 (2004) 349.
- [2] M. Luiz, A. Biasutti, A.T. Soltermann, N.A. Garcia, Polymer Degrad. Stab. 63 (1999) 447.
- [3] N. Noma, S. Yamazaki, N. Tohge, J. Sol–Gel. Sci. Technol. 31 (2004) 253.
- [4] E. Kwiatkowski, G. Romanowski, W. Nowicki, M. Kwiatkowski, K. Suwińska, Polyhedron 22 (2003) 1009.
- [5] E. Kwiatkowski, G. Romanowski, W. Nowicki, M. Kwiatkowski, Polyhedron 25 (2006) 2809.
- [6] E. Kwiatkowski, G. Romanowski, W. Nowicki, M. Kwiatkowski, K. Suwińska, Polyhedron 26 (2007) 2559.
- [7] G.M. Sheldrick, Acta Crystallogr., Sect A 46 (1990) 467.
- [8] G.M. Sheldrick, SHELXL-NT Version 6.12, University of Gottingen, Germany, 2000.
- [9] A.R. Katritzky, Y.J. Xu, H.Y. He, S. Mehta, J. Org. Chem. 66 (2001) 5590.
- [10] A. Habtemariam, B. Watchman, B.S. Potter, R. Palmer, S. Parsons, A. Parkin, P.J. Sadler, J. Chem. Soc., Dalton Trans. (2001) 1306.
- [11] A. Khanna, A. Bala, B.L. Khandelwal, J. Organomet. Chem. 494 (1995) 199; A.K. Singh, V. Srivastava, Phosphorus Sulfur Silicon 47 (1990) 471.
- [12] (a) P.E. Garrou, Chem. Rev. 82 (1982) 229; (b) A.K. Singh, S. Sharma, Coord. Chem. Rev. 209 (2000) 49; (c) E.G. Hope, W. Levason, Coord. Chem. Rev. 122 (1993) 109; (d) W. Levason, D. Orchard, G. Reid, Coord. Chem. Rev. 225 (2002) 159.
- [13] R. Kumar, S. Upreti, A.K. Singh, Polyhedron 27 (2008) 1610.
- [14] (a) A. Kumar, M. Agarwal, A.K. Singh, Polyhedron 27 (2008) 485; (b) I.D. Kostas, B.R. Steele, A. Terzis, S.V. Amosova, A.V. Martynov, N.A. Makhavaeva, Eur. J. Inorg. Chem. (2006) 2642.
- [15] R. Kumar, A.K. Singh, R.J. Butcher, P. Sharma, R.A. Toscano, Eur. J. Inorg. Chem. (2004) 1107.

- [16] K.D. Dimitra, P.N. Yadav, M.A. Demertzis, J.P. Jasiski, F.J. Andreadakic, I.D. Kostas, *Tetrahedron Lett.* 45 (2004) 2923.
- [17] A.K. Singh, C.V. Amburose, M. Mishra, R.J. Butcher, *J. Chem. Res. (S)* (1999) 716.
- [18] G. Tresoldi, G. Bruno, P. Piraino, G. Faraone, G. Bombieri, *J. Organomet. Chem.* 265 (1984) 311.
- [19] A.J. Carty, P.C. Chieh, N.J. Taylor, W.T. Wong, S. Yau, *J. Chem. Soc., Dalton Trans.* (1976) 572.
- [20] R. Kumar, P.A.K. Singh, J.E. Drake, M.B. Hursthouse, M.E. Light, *Inorg. Chem. Commun.* 7 (2004) 502.
- [21] L-B. Han, N. Choi, M. Tanaka, *J. Am. Chem. Soc.* 118 (1996) 7000.
- [22] A.J. Canty, M.C. Denney, J. Patel, H. Sun, B.W. Skelton, A.H. White, *J. Organomet. Chem.* 689 (2004) 672.
- [23] A.K. Singh, J. Sooriyakumar, J.E. Drake, M.B. Hursthouse, M.E. Light, *J. Organomet. Chem.* 613 (2000) 244.
- [24] A.K. Singh, J. Sooriyakumar, S. Husebye, K.W. Tornroos, *J. Organomet. Chem.* 612 (2000) 46.
- [25] C.S. Slone, D.A. Weinberger, C.A. Mirkin, *Prog. Inorg. Chem.* 48 (1999) 233; A. Borner, *Eur. J. Inorg. Chem.* (2001) 327.
- [26] I.G. Jung, S.U. Son, K.H. Park, K.-C. Chung, J.W. Lee, Y.K. Chung, *Organometallics* 22 (2003) 4715; E. Diez-Barra, J. Guerra, V. Hornillos, S. Merino, Tejada, *J. Organomet.* 22 (2003) 4610–4612; C.S. Consorti, M.L. Zanini, S. Leal, G. Ebeling, J. Dupont, *Org. Lett.* 5 (2003) 83; J. Masllorens, M. Moreno-Mañas, A. Pla-Quintana, A. Roglans, *Org. Lett.* 5 (2003) 1559; S.B. Park, H. Alper, *Org. Lett.* 5 (2003) 3209; C. Mazet, L.H. Gade, *Eur. J. Inorg. Chem.* (2003) 1161.
- [27] Q. Yao, E.P. Kinney, C. Zheng, *Org. Lett.* 6 (2004) 2999.
- [28] N. Miyaura, A. Suzuki, *Chem. Rev.* 95 (1995) 2457; A.F. Littke, G.C. Fu, *Angew. Chem., Int. Ed.* 41 (2002) 4176; R.B. Bedford, C.S.J. Cazin, D. Holder, *Coord. Chem. Rev.* 248 (2004) 2283.
- [29] F.Y. Kwong, W.H. Lam, C.H. Yeung, K.S. Chan, A.S. C Chan, *Chem. Commun.* (2004) 1922–1923; J. Zhou, G.C. Fu, *J. Am. Chem. Soc.* 126 (2004) 1340; I.J.S. Fairlamb, A.R. Kapdi, A.F. Lee, *Org. Lett.* 6 (2004) 4435; C. Baillie, L. Zhang, J.J. Xiao, *Org. Chem.* 69 (2004) 7779.